Melanie Pertl, BSc.

Effect of Shuttling Protein Depletion on Early Pre-ribosome Maturation

MASTER'S THESIS

to achieve the university degree of

Master of Science

Master's degree programme: Molecular Microbiology

submitted to

Graz University of Technology

Supervisor

Ao. Univ.-Prof. Dr. Helmut Bergler

Institute of Molecular Biosciences

Graz, March 2017

AFFIDAVIT

I declare that I have authored this thesis independently, that I have not used other than the declared sources/resources, and that I have explicitly indicated all material which has been quoted either literally or by content from the sources used. The text document uploaded to TUGRAZonline is identical to the present master's thesis dissertation.

24.3.2017
Date

Signature

Ein herzliches Dankeschön

an Helmut Bergler für die Möglichkeit an diesem Projekt zu arbeiten, sowie seine großartige Betreuung während dieser Arbeit.

an Gertrude Zisser für die ganzen tollen Tipps und immer für alle meine Anliegen da zu sein.

an alle Mitglieder der Bergler/Pertschy Arbeitsgruppe, die mich so herzlich in ihre Mitte aufgenommen und ein sehr gutes Arbeitsklima geschaffen haben.

an Michi für die tatkräftige Unterstützung in allen Lebenslagen und viele schöne Stunden.

an meine Familie: Susanne, Christoph, Lisa, Valentina für die geborgene Umgebung in der ich aufwachsen und mich zu dem Menschen entwickeln durfte, der ich jetzt bin.

an meine langjährigen Freundinnen Ria, Nina, Moni, Kerstin dafür, immer an mich zu glauben und mich in allem was ich mache zu bestärken.

Zusammenfassung

Für das Wachstum und Überleben von allen Zellen sind Proteine essentielle Biomoleküle. Sie werden von Ribosomen hergestellt, Nanomaschinen die in allen Lebewesen hochkonserviert vorliegen. Die Bäckerhefe *Saccharomyces cerevisiae* ist ein sehr geeigneter Modellorganismus um die molekularen Mechanismen und Prozesse hinter der Biogenese von Ribosomen zu untersuchen.

Eukaryotische 80S Ribosomen bestehen aus einer kleinen 40S und einer großen 60S Untereinheit. Ribosomenbiogenese beginnt im Nukleolus mit der Transkription einer Vorläufer-rRNA. Durch die Assemblierung einer Vielzahl von Proteinen mit dieser prä-rRNA wird ein großer Komplex gebildet, der als 90S prä-Ribosom bezeichnet wird. Innerhalb dieses Komplexes wird die rRNA mehrfach prozessiert was unter anderem die Vorläuferpartikel der 40S von der 60S Untereinheiten trennt.

Indem man Hefezellen mit dem Wirkstoff Diazaborin behandelt, wird die Ablösung von Shuttle Proteinen von prä-60S Partikeln kurz nach deren Export ins Zytoplasma inhibiert und damit deren Rückführung in den Zellkern verhindert. Dadurch werden die Shuttle Proteine im Zellkern depletiert und frühe Reifungsschritte der prä-Ribosomen inhibiert.

Die vorliegende Arbeit wurde erstellt um zu untersuchen wie sich der Abbau von bestimmten Shuttle Proteinen durch das AID System auf die Zusammensetzung früher prä-ribosomaler Partikel auswirkt. Dabei wird ein spezieller tag an das jeweilige Shuttle Protein fusioniert, der in Anwesenheit von Auxin zu einer raschen Degradation des Proteins führt. Dabei wurde gefunden, dass bereits durch die Fusion des tags an manche Shuttle Proteine die Zusammensetzung früher Partikel verändert wird. Zusätzlich wurde durch „yeast two hybrid“ Untersuchungen eine mögliche Interaktion zwischen frühen 90S Faktoren und Shuttle Proteinen untersucht.

Abstract

Proteins are essential biomolecules needed for growth and survival of living cells. They are synthesized by ribonucleoprotein nano-machines called ribosomes. Ribosomes are highly conserved throughout all organisms which makes the yeast *Saccharomyces cerevisiae* a suitable model organism to investigate the molecular processes and mechanisms behind their biogenesis.

Eukaryotic 80S ribosomes consist of a large 60S subunit and a small 40S subunit. Their biogenesis starts in the nucleolus with the transcription of a large pre-rRNA. The assembly of numerous protein components to this pre-rRNA results in the formation of a huge complex called the 90S pre-ribosome. Within this complex the pre-rRNA is processed and cleaved resulting in the formation of pre-40S and pre-60S particles which are the precursors of the small and large subunit, respectively. Treating yeast cells with the compound diazaborine leads to an inhibition of ribosome biogenesis by trapping shuttling proteins in the cytoplasm. Their retention in the cytoplasm leads to an inhibition of early pre-ribosome maturation steps in the nucleolus.

This study aimed to investigate how the degradation of individual shuttling proteins using the AID system affects the composition of early pre-ribosomal particles. This system involves the fusion of a degradation tag to the protein of interest and allows its rapid degradation in the presence of auxin. We could show that the C-terminal tagging of selected shuttling proteins interferes with the composition of early pre-ribosomal particles suggesting that shuttling proteins play a role in early maturation steps. In addition, a possible *in vivo* interaction between shuttling proteins and selected early pre-60S maturation factors was investigated.

Contents

1. Introduction

Ribosomes are ribonucleoprotein nano-machines that translate mRNA and catalyze protein synthesis in all organisms. In yeast, 80S ribosomes consist of two subunits, the small 40S subunit containing 18S ribosomal RNA and 33 ribosomal proteins and the large 60S subunit which consists of 5S, 5.8S and 25S rRNA as well as 46 ribosomal proteins. For the correct assembly of ribosomes with these rRNAs and ribosomal proteins more than 200 non-ribosomal assembly factors and 76 different small nucleolar RNAs (snoRNAs) are needed. These trans-acting factors associate transiently with nascent ribosomes on their way from the nucleolus to the cytoplasm ensuring their correct assembly and function. This is a highly complex and well organized process considering that more than 2000 ribosomes are assembled each minute [Woolford & Baserga, 2013].

1.1. Ribosome biogenesis in *Saccharomyces cerevisiae*: an overview

Ribosome biogenesis starts in the nucleolus, a non-membrane surrounded sub-compartment of the cell. There, RNA polymerase I transcribes the 35S pre-rRNA (primary transcript) that is processed to mature 18S, 5.8S and 25S rRNA. This transcription takes up 60% of the total RNA transcription in the cell [French, et al., 2003; Kos & Tollervey, 2010]. 5S rRNA is transcribed by RNA polymerase III in the opposite direction [Warner, 1999]. The 35S primary transcripts contain internal and external transcribed spacer sequences (ITS, ETS) that are removed co-transcriptionally by endo- and exonucleolytic cleavage during ribosome assembly. These cleavages can occur in the A0, A1 or A2 site. Cleavage in the A0 site generates 33S pre-rRNA and subsequent processing in the A1 site generates 32S pre-rRNA [Beltrame, et al., 1994]. Cleavage at the A2 site in ITS1 results in generating the 20S and $27SA_2$ pre-rRNA (Figure 1). This event splits the 90S particle into 40S and 60S pre-ribosomal subunits which then independently run through further processing on their way to the cytoplasm [Udem & Warner, 1972; Venema & Tollervey, 1995].

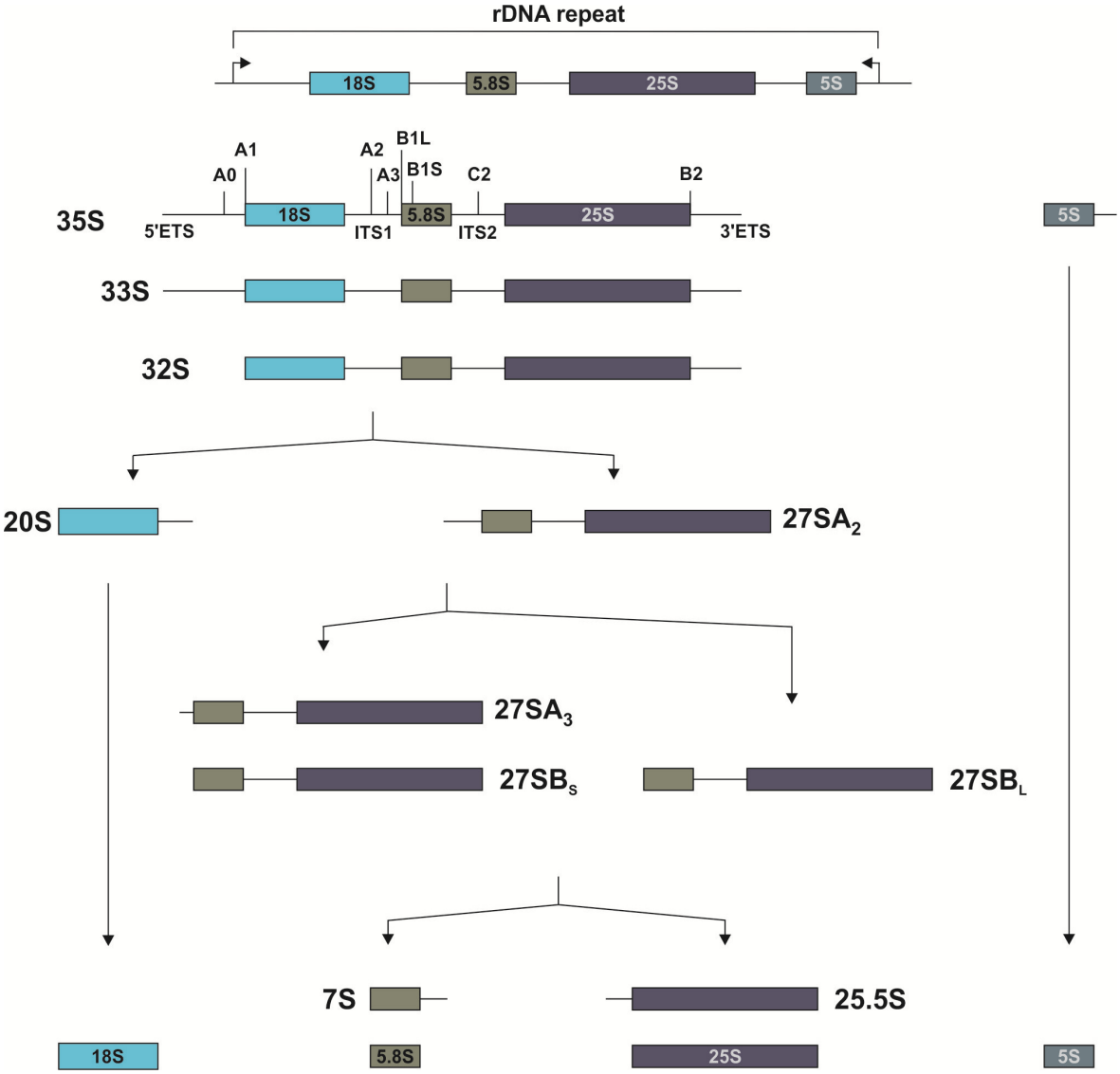

Figure 1: Overview of rRNA processing in *S. cerevisiae*. About 150 rDNA repeats are localized on the yeast chromosome XII. Each repeat contains sequences for ribosomal rRNAs of the small and large ribosomal subunit. In the nucleolus the 18S, 5.8S and 25S rRNA are transcribed by RNA polymerase I as a common 35S precursor rRNA. In the opposite direction RNA polymerase III transcribes the 5S rRNA which is then processed in an independent way. The 35S rRNA contains internal (ITS) and external (ETS) spacer sequences. They are cleaved by exo- and endonucleolytic processes. After cleavage in A2 the 20S rRNA is directly transported into the cytoplasm where the mature 18S rRNA is produced. The 60S subunit precursor rRNA $27SA_2$ is processed by two independent pathways both resulting in the formation of mature 5.8S and 25S rRNAs in the cytoplasm.

The 20S pre-rRNA is than packed in 43S particles. These 43S pre-rRNPs are exported from the nucleolus through the nucleoplasm to the cytoplasm, where the 20S pre-rRNA undergoes final endonucleolytic cleavage by Nob1, producing mature 18S rRNA [Fatica, et al., 2003; Pertschy, et al., 2009].

The maturation of 60S pre-ribosomes takes more time. About 90% of $27SA_2$ rRNA is processed by the major pathway. The 5' end of the $27SA_2$ is processed in site A3 by the RNAse MRP (mitochondrial RNA processing) to form the shorter $27SA_3$ rRNA. Exonucleases Rat1 and Rrp17 then remove the remaining ITS1 spacer sequence to form $27SB_S$ rRNA [Lygerou, et all., 1996; Oeffinger, et all., 2009; Woolford& Baserga, 2013]. The minor pathway directly results in the formation of $27SB_L$ by cleavage in the B1L site without formation of the $27SA_3$ intermediate. $27SB_S$ and $27SB_L$ then undergo the same nucleoplasmatic cleavage in the C2 site of spacer ITS2 generating 25.5S and 7S pre-rRNA (Figure 1). Several subsequent processing steps of the 25.5S and 7S pre-rRNAs take place in the cytoplasm and result in formation of mature 25S and 5.8S rRNA. Mature 40S and 60S subunits join to form the 80S ribosome and enter the pool of functioning ribosomes in the cytoplasm (Figure 2) [Gasse, et al., 2015; Henry, et al., 1994; Mitchell, et al., 1996; Geerlings, et al., 2000; Woolford & Baserga, 2013].

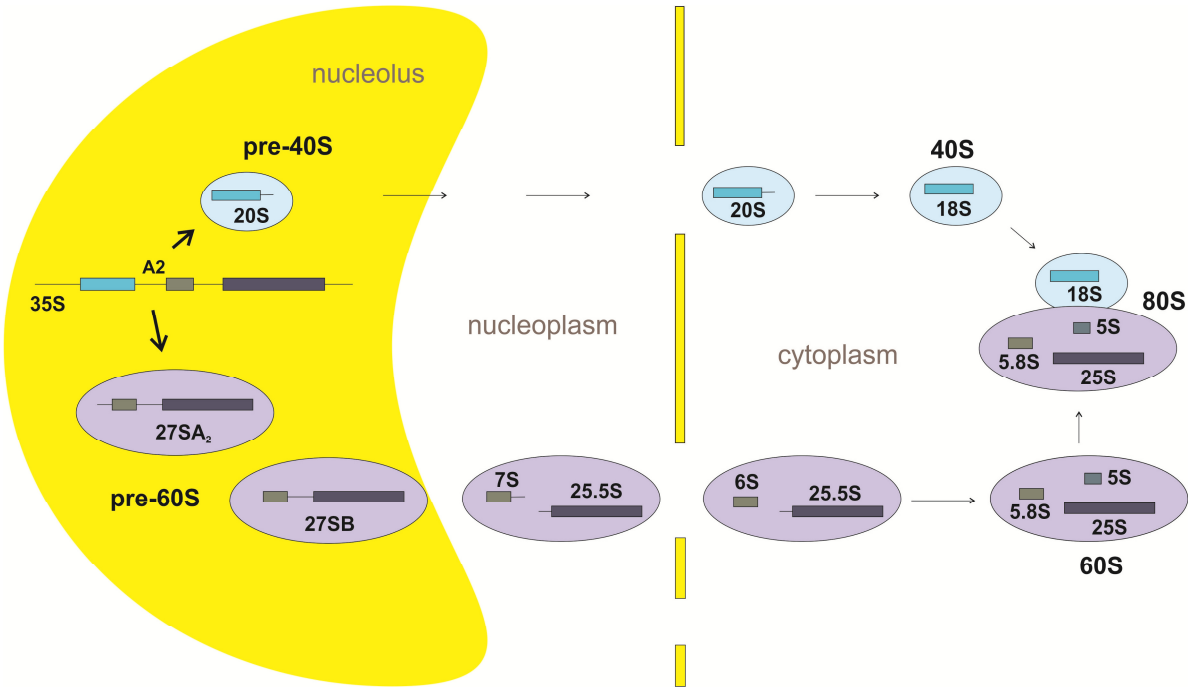

Figure 2: Maturation pathway of pre-ribosomal particles. After several processing reactions at the 5' end, the 32S pre-rRNA is endonucleolytically cleaved at site A2. After that cleavage the 20S rRNA is packed into pre-40S particles. They are directly transported from the nucleolus to the cytoplasm. In contrast, the $27SA_2$ is packed into pre-60S particles which undergo numerous steps of rRNA processing as well as continuous assembly and disassembly of non-ribosomal factors ensuring correct folding on their way to the cytoplasm. In the cytoplasm final maturation steps occurs until the large and small subunits can assemble to the 80S ribosomes.

1.2. Co-transcriptional cleavage of pre-rRNA depends on the presence of U3 snoRNA and results in the formation of 20S and 27SA$_2$ rRNA

Already during transcription of the 35S pre-rRNA numerous trans-acting factors and early binding ribosomal proteins of the small subunit assemble to the rRNA which results in formation of a large complex called the 90S pre-ribosome or small-subunit (SSU) processome. Most of the non-ribosomal factors of the SSU assembly machinery are called U three proteins. The most important snoRNA in this complex is the box C/D snoRNA U3 [Dragon, et al., 2002]. Box C/D snoRNPs contain the protein components Nop1, Nop58, Nop56 and Snu13. Together with a snoRNA which allows proper base pairing between the snoRNP and the pre-rRNA they carry out 2'-O-ribose methylation [Dutca, et al., 2011; Osheim, et al., 2004; Kornprobst, et al., 2016]. The U3 snoRNA however is not involved in methylation but functions as a chaperone and is essential for SSU processome assembly. It binds to the 5'ETS of the 35S rRNA and two sites of the 18S rRNA. The 90S pre-ribosome is then assembled from a 5' to 3' direction in a complex manner. Important for the binding of the U3 to the 35S pre-rRNA is the U3 specific protein Rrp9 which does not assemble to other box C/D snoRNAs [Chaker-Margot, et al., 2016; Zhang, et al., 2013; Sun, et al., 2017].

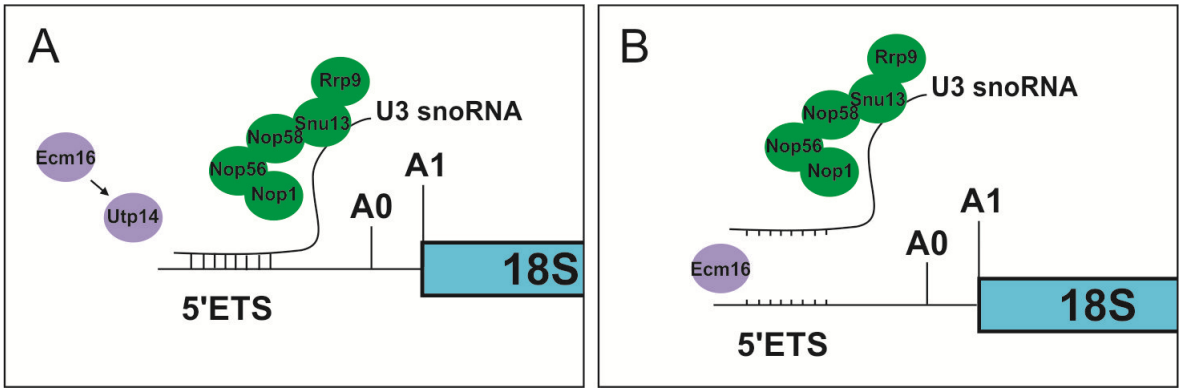

Figure 3: U3 snoRNP is essential for 90S pre-ribosome formation. A The box C/D U3 snoRNP consists of the U3 snoRNA and protein components: Nop1, Nop56, Nop58, Snu13, and the U three specific Rrp9. The U3 snoRNA basepairs with the 35S pre-rRNA to promote its correct folding and processing within the SSU processome. Utp14 recruits the RNA helicase Ecm16 to the pre-ribosome. **B** After activation by Utp14, Ecm16 unwinds U3 from the pre-ribosome to promote formation of the central pseudoknot and further processing and maturation.

To allow the following formation of the central pseudoknot as well as other subsequent maturation steps, the U3 snoRNA needs to be removed. Utp14 is supposed to recruit and activate the RNA helicase Ecm16 (also called Dhr1) to undock the U3 snoRNA from the pre-ribosome (Figure 3) [Zhu, et al., 2016; Sardana, et al., 2015].

Separation of the 40S and 60S from 90S pre-ribosomes can either occur co-transcriptionally by cleaving the A0-A2 site or post-transcriptionally by cleavage in the A3 site [Turowski & Tollervey, 2015]. In rapidly growing yeast cells co-transcriptional processing takes up about 80% [Talkish, et al., 2016]. The RNA cyclase-related protein Rcl1 is proposed to carry out the cleavage in A2 generating the 20S and $27SA_2$ (Figure 1) [Horn, et al., 2011].

Post-transcriptional cleavage in A3 is carried out by the RNase MRP and results in formation of the 23S and $27SA_3$ (Figure 4) [Lygerou, et al., 1996].

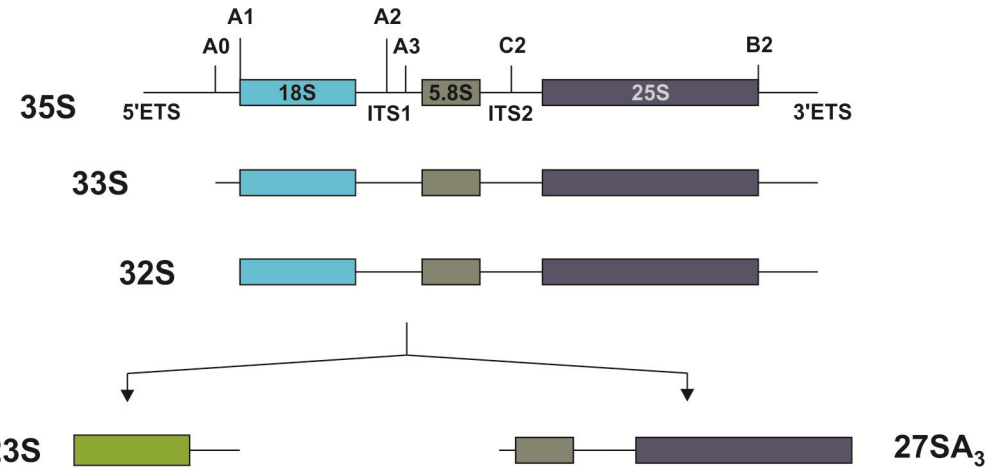

Figure 4: Post-transcriptional cleavage of the 32S pre-rRNA in the A3 site by MRP results in formation of 23S and $27SA_3$. Disruption of ribosome assembly due to a range of external and internal factors leads to an increase of cells producing 23S rRNA populations. This is explained by a shift from co- to post-transcriptional cleavage in A3 which occurs if cells are in distress.

According to Talkish, et al. [2016] increasing cell density as well as treating yeast cells with different substances leads to a disruption of ribosome assembly

and therefore a disturbance in the hierarchy of rRNA processing. The cells shift from a co-transcriptional cleavage to a post-transcriptional population rather containing 23S rRNA, leading to a decreasing amount of 20S rRNA.

1.3. Diazaborine treatment leads to defects in early steps of ribosome biogenesis

In eukaryotes, 60S ribosome biogenesis is depending on shuttling proteins (i.e. Rlp24, Nog1, Tif6 and Mrt4). They bind to pre-60S particles in the nucleolus and accompany them through the nucleoplasm into the cytoplasm where they have to be released and recycled into the nucleolus [Saveanu, et al., 2003; Panse & Johnson, 2010]. The AAA-ATPase Drg1 assembles to pre-ribosomes after their export through the nuclear pore complex and triggers the release of Rlp24 and Nog1 by ATP hydrolysis [Kappel, et al., 2012]. This is a prerequisite for the release of the other shuttling factors Mrt4 and Tif6 (schematically depicted in Figure 5A). Mrt4 acts as a placeholder for the ribosomal stalk protein P0 (Rpp0) and is supposed to be released in the cytoplasm by Yvh1. As a late step of maturation, Tif6 is released from the particle with help of the GTPase Efl1 and its guanine nucleotide exchange factor Sdo1 and is recycled into the nucleolus. Deletion of Yvh1 leads to the accumulation of Mrt4 as well as Tif6 in the cytoplasm indicating that assembly and disassembly of shuttling factors is regulated in a timely manner. [Pertschy, et al., 2007 ; Senger, et al., 2001 ; Kemmler, et al., 2009 ; Lo, et al., 2009 ; Lo, et al., 2010]. A recent publication proposed that the release of Mrt4 by Yvh1 already takes place in the nucleus revealing a binding site for the Mex67-Mtr2 export factor complex [Sarkar, et al., 2016].

The drug diazaborine is the first compound to be discovered as an inhibitor of ribosome biogenesis in yeast [Pertschy, et al., 2004]. Treating yeast cells with diazaborine inactivates the AAA-ATPase Drg1 and therefore blocks the release of Rlp24 from pre-ribosomes [Loibl, et al., 2014]. As a consequence, the other shuttling proteins cannot be released and recycled back into the nucleolus. This leads to their retention in the cytoplasm and subsequent depletion in the nucleus

causing a blockage of very early pre-60S maturation steps (Figure 5B) [Senger, et al., 2001; Jensen, et al., 2003; Lo, et al., 2010].

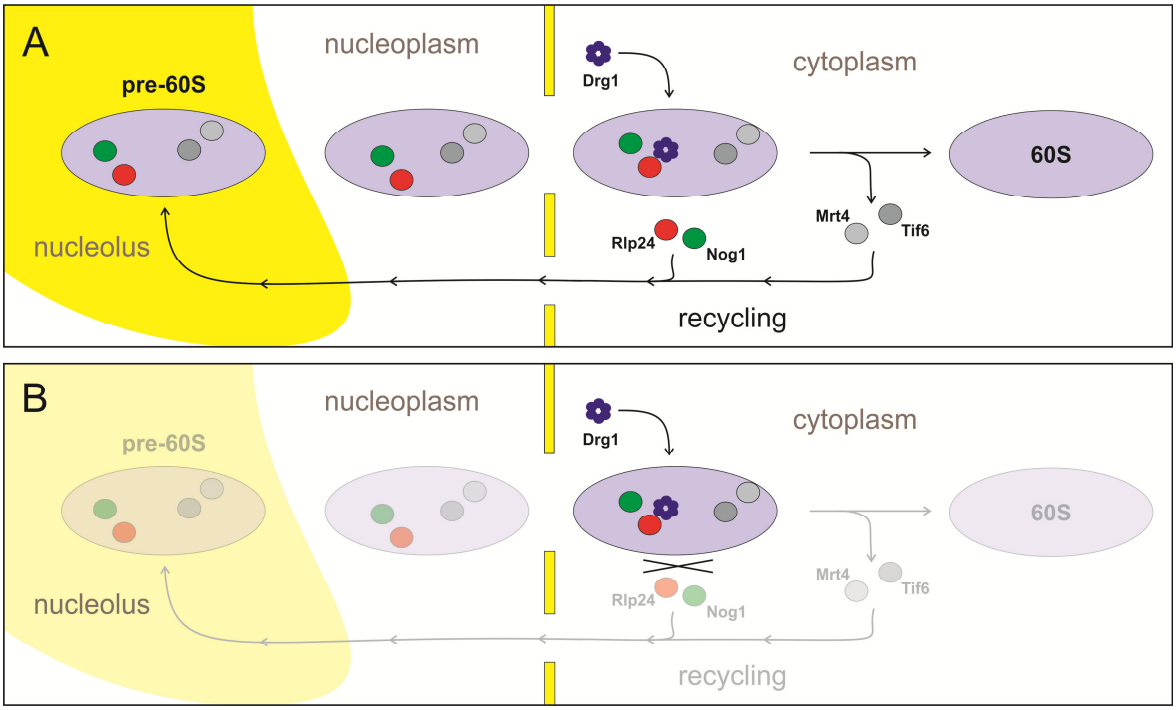

Figure 5: 60S biogenesis is depending on shuttling proteins. A Shuttling proteins bind to pre-60S ribosomal subunits in the nucleolus and accompany the particles through the nucleoplasm into the cytoplasm. In the cytoplasm the release of Rlp24 and Nog1 by the AAA-ATPase Drg1 is required for the downstream release of Mrt4 and Tif6. Shuttling protein release is required for their recycling into the nucleolus where they bind to newly made pre-60S particles and perform the next round of action. **B** Diazaborine treatment blocks the release of shuttling proteins in the cytoplasm by inhibiting the ATPase activity of Drg1. As a consequence, shuttling proteins accumulate in the cytoplasm and are depleted in the nucleus which disrupts early pre-ribosomal maturation steps.

Tandem affinity purification (TAP) using Nop58-TAP as bait protein allowed novel insides into the effect of shuttling protein depletion on early pre-60S particles (Zisser, G; unpublished data). As shown in Figure 6B already after 5 minutes of diazaborine treatment an accumulation of 32S rRNA occurs. This indicates a fast inhibition of the cleavage at A2 after depletion of shuttling proteins induced by diazaborine treatment.

The decrease of $27SA_2$ and 20S species in the northern blot confirms this assumption. If the cleavage in A2 cannot occur, a cleavage in the A3 site producing 23S and $27SA_3$ often occurs as a consequence. An increase of 23S rRNA species in the northern blot indeed shows that this also happens after diazaborine treatment.

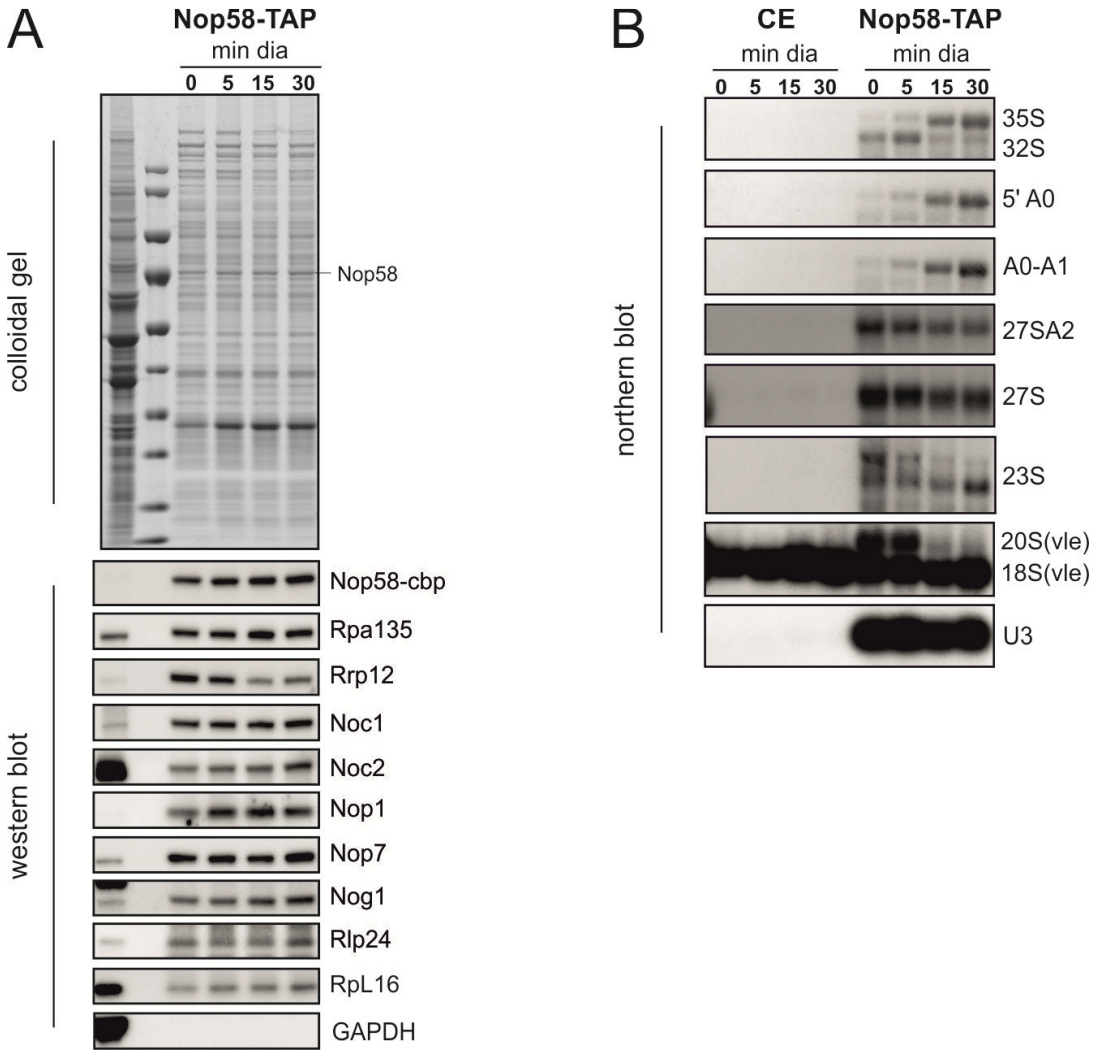

Figure 6: Tandem affinity purification of Nop58 containing ribosomal particles upon diazaborine treatment. Prior to purification, the cells were treated with 100 µg/ml diazaborine for different time frames. In **A** the colloidal coomassie blue stained 4-12% polyacrylamide gradient gel is shown (marker: PageRuler prestained protein ladder, Thermo scientific) as well as the western blot. Different antibodies directed against 90S and 60S factors were used to analyse the protein composition of the purified particles. The bait protein Nop58 was detected with an antibody directed against the calmodulin binding protein (cbp). In **B** the analysis of the RNA species is show by northern blotting (Zisser, G. & Mitterer, V.; unpublished results). Vle: very long exposure.

By having a look at the western blot in Figure 6A changes of the protein composition of Nop58 containing particles can be observed upon diazaborine treatment. Rrp12 is present on the 90S pre-ribosome and proposed to bind in the 3' major domain of pre-rRNA after Noc2 has already bound [Chaker-Margot, et al., 2015]. A decrease of Rrp12 on Nop58 particles indicates a blockage in processing steps before the protein is able to bind. Noc2 has already assembled to the pre-ribosome and might not be released anymore since it accumulates on Nop58 particles. The particles shift to an earlier population of pre-ribosomes not able to further mature due to defects in early processing steps.

As diazaborine treatment traps shuttling factors in the cytoplasm, these data indicate that the blockage in release and recycling of shuttle proteins leads to an immediate disturbance of very early maturation steps and their possible involvement in 90S processing.

1.4. Aim of this study

Based on previous findings in our laboratory the aim of this study was to find a technique which allows the rapid depletion of individual shuttling proteins. This should be accomplished by using an auxin inducible degron (AID) system. It allows a rapid degradation of proteins of interest (POI's) fused to an AID tag [Nishimura, et al., 2009]. Into strains in which individual shuttling proteins contain an AID tag (provided by Fasching, S; unpublished data) a TAP tag should be integrated in frame with Nop58 to allow purification of early pre-ribosomal particles. After shuttling protein depletion by auxin treatment, alteration in early particle composition upon degradation of Mrt4, Tif6, Nog1, Rlp24 should be investigated.
Additionally a possible interaction of these shuttling factors with early 90S factors (Utp14, Ecm16) should be investigated using the yeast two hybrid system [James, et al., 1996].

2. Materials and methods

2.1. Strains and plasmids

Table 1: List of strains used in this study.

strains	genotype	source & reference	IMB No.
Escherichia coli XL-1 blue	*endA1 hsdR17 relA1 D(lac) supE44 thi1 lrecA1 gyrA96 [F´proAB laclq ZΔM15 Tn10 (tetr)]*	Stratagene	#3771
Saccharomyces cerevisiae			
PJ69-4A	*MAT*a *trp1-901 leu2-3,112 ura3-52 his3-200 gal4Δ gal80Δ LYS::GAL1-HIS3 GAL2-ADE2 met2::GAL7-lacZ*	Kressler, D; University of Fribourg [James et al., 1996]	Pertschy collection #1040
Y5159	*MAT*α *leu2 ura3 his3 ade2 trp1 PADH1-OsTIR1-9Myc::TRP*	Hurt, E; University of Heidelberg [Nishimura et al., 2009]	Pertschy collection #2601
Y5159; Tif6-AID-Flag	See Y5159; *TIF6-AID-Flag::HISMX6*	Sandra Fasching	#6629C
Y5159; Mrt4-AID-Flag	See Y5159; *MRT4-AID-Flag::HISMX6*	Sandra Fasching	#6629B
Y5159; Nog1-AID-Flag	See Y5159; *NOG1-AID-Flag::HISMX6*	Sandra Fasching	#6629D
Y5159; Rlp24-AID-Flag	See Y5159; *RLP24-AID-Flag::HISMX6*	Sandra Fasching	#6630A
Y5159; Nop58-TAP; Utp14-3xHA	See Y5159; *Nop58-TAP; Utp14-3xHA*	this study	#6631A
Y5159; Tif6-AID-Flag; Nop58-TAP; Utp14-3xHA	See Y5159; *TIF6-AID-Flag::HISMX6 NOP58-TAP::KanMX6 UTP14-3xHA::NatNT2*	this study	#6631B
Y5159; Mrt4-AID-Flag; Nop58-TAP; Utp14-3xHA	See Y5159; *MRT4-AID-Flag::HISMX6 NOP58-TAP::KanMX6 UTP14-3xHA::NatNT2*	this study	#6631C
Y5159; Nog1-AID-Flag; Nop58-TAP; Utp14-3xHA	See Y5159; *NOG1-AID-Flag::HISMX6 NOP58-TAP::KanMX6 UTP14-3xHA::NatNT2*	this study	#6631D
Y5159; Rlp24-AID-Flag; Nop58-TAP; Utp14-3xHA	See Y5159; *RLP24-AID-Flag::HISMX6 NOP58-TAP::KanMX6 UTP14-3xHA::NatNT2*	this study	#6632A

Table 2: List of plasmids used in this study

plasmid	features	source
pFA6a-TAP-kanMX	TAP-tag; kanMX6; Amp^R	Brigitte Pertschy
pFA6a-3xHA-natNT2	3x HA-tag; natNT2; Amp^R	Brigitte Pertschy
pGAD-C1	P.ADH1; GAL4AD; *LEU2*; Amp^R	Philipp James
pGBDU-C1	P.ADH1; GAL4DBD; *URA3*; Amp^R	Philipp James
pGBDU-C1-*MRT4*	P.ADH1; GAL4DBD-Mrt4; *URA3*; Amp^R	this study
pGBDU-C1-*TIF6*	P.ADH1; GAL4DBD-Tif6; *URA3*; Amp^R	this study
pGBDU-C1-*RLP24*	P.ADH1; GAL4DBD-Rlp24; *URA3*; Amp^R	this study
pGBDU-C1-*NOG1*	P.ADH1; GAL4DBD-Nog1; *URA3*; Amp^R	this study
pGAD-C1-*UTP14*	P.ADH1; GAL4AD-Utp14; *LEU2*; Amp^R	this study
pGAD-C1-*ECM16*	P.ADH1; GAL4AD-Ecm16; *LEU2*; Amp^R	this study
pGBDU-C1-*MTR4*	P.ADH1; GAL4DBD-Mtr4; *URA3*; Amp^R	this study
pGAD-C1-*NOP53*	P.ADH1; GAL4AD-Nop53; *LEU2*; Amp^R	this study

2.2. Media and growth conditions

Yeast strains used in this study were grown in YPD complex medium or SD (synthetic dextrose complete) medium (Table 3) supplemented with amino acids (Table 4).

Table 3: Media for yeast cultivation

medium	component	concentration [g/l]
YPD complex medium	yeast extract	10
	peptone	20
	2% glucose	20
	agar (optional)	15-20
	pH 5.5	
SD synthetic dextrose complete medium	solution A (pH 5.5):	
	yeast nitrogen base	1.4
	$(NH_4)_2SO_4$	5
	solution B	
	2% glucose	20
	agar (optional)	20
	amino acid mix	1x

For solid media, agar was added to the media components as outlined in Table 3. Solutions A and B of SD media were autoclaved separately and then mixed and supplemented with a sterile amino acid mix. When using selection markers natNT2 and kanMX6, YPD medium was supplemented with 100 µg/ml ClonNat (natNT2) or 300 µg/ml Geneticin (kanMX) after sterilisation. If not indicated otherwise yeast incubation temperature was set for 30°C, agitation for 170 rpm.

Table 4: Composition of the supplemented amino acid mix for SD media

amino acid	final concentration [mg/l]	10x mix [g/l]
adenine sulfate	20	0.2
uracil	20	0.2
L-tryptophan	20	0.2
L-histidine-HCl	20	0.2
L-arginine-HCl	20	0.2
L-methionine	20	0.2
L-tyrosine	30	0.3
L-leucine	30	0.3
L-isoleucine	30	0.3
L-lysine-HCl	30	0.3
L-phenylalanine	50	0.5
L-glutamic acid	100	1.0
L-aspartartic acid	100	1.0
L-valine	150	1.5
L-threonine	200	2.0
L-serine	400	4.0

Bacterial strains were grown in 2xTY medium (Table 5) supplemented with 100 µg/ml ampicillin if needed for plasmid maintenance. If not indicated otherwise incubation temperature was set for 37°C, agitation for 170 rpm.

Table 5: Growth media for *E. coli* cultivation

media	component	concentration [g/l]
2xTY	tryptone	16
	yeast extract	10
	NaCl	5
	agar (optional)	15
	pH 7.5	

2.3. Oligonucleotides

The primers in this study were purchased from Sigma Aldrich and are listed in Table 6.

Table 6: List of oligonucleotides used in this study

primer name	primer sequence (5'-3')	info
Mrt4_fwd_BamHI	TATAGGATCCATGCCAAGATCAAAACGTTCC	cloning*
Mrt4_rev_SalI	TATAGTCGACTTATTCCATGTTGATGTTAGTGCTTTC	cloning*
Tif6_fwd_BamHI	TAGCGGATCCATGGCTACCAGGACTC	cloning*
Tif6_rev_XhoI	GATCCTCGAGCTATGAGTAGGTTTCAAT	cloning*
Rlp24_fwd_BamHI	TATATGGATCCATGAGAATTTATCAATGCCATTTTTG	cloning*
Rlp24_rev_SalI	TATATGTCGACCTAAAAAGCAATTTTCTTTGTATTTCTTC	cloning*
Nog1_fwd_BamHI	TATAGGATCCATGCAACTTTCATGGAAGG	cloning*
Nog1_rev_SalI	TATAGTCGACTCAACGGAAATCTGTCTTACC	cloning*
Utp14_fwd_SmaI	TATACCCGGGATGGCAAAAAAGAAATCTAAGAGCAG	cloning*
Utp14_rev_XhoI	TATACTCGAGTTACTTAAATGGTGCCTTCAAAGG	cloning*
Ecm16_fwd_SmaI	TATACCCGGGATGGGTACTTACAGAAAAAGGTTTA	cloning*
Ecm16_rev_XhoI	TATACTCGAGTTATTTTTTTCCTTTCTCTTCACCTG	cloning*
Nop53_fwd_BamHI	TATAGGATCCATGGCTCCAACTAATCTAACCAAG	cloning*
Nop53_rev_XhoI	TATACTCGAGCTATTTGAAGTCCTTATGTGTCCAC	cloning*
Mtr4_fwd_EcoRI	TATAGAATTCATGGATTCTACTGATCTGTTCGATGTTTT	cloning*
Mtr4_rev_SalI	TATATGTCGACCTATAAATACAAAGAACCAGCAGATAC GA	cloning*
Nop58_F2_fwd	AGAAAGAGAAGAAGGAAAAGAAGTCCAAGAAAGAGAA GAAAGAGAAGAAA**CGGATCCCCGGGTTAATTAA**	tagging*
Nop58_S2_rev	AGGGAACGCGAGGGGTCACTAATTATTAAAATGTAAAA TGCATCC**ATCGATGAATTCGAGCTCG**	tagging*
Utp14_F2_fwd	GACTAAGCCAGGCCAAGTTATTGATCCTTTGAAGGCAC CATTTAAG**CGGATCCCCGGGTTAATTAA**	tagging*
Utp14_S2_rev	GTGGAATGTGCCACATATGCATTTTTTTACCACCAATAA ATATCAG**ATCGATGAATTCGAGCTCG**	tagging*
Nop58_CTRL-fwd	TCTCTTGTTGGTCAAGCTAC	colony PCR
Utp14_CTRL-fwd	CGTGTCATTGATGATGAAG	colony PCR
Kan5'b_CTRL-rev	CAAGACTGTCAAGGAGGG	colony PCR reverse primer

* Recognition sites of restriction endonucleases are underlined. Bold letters indicate the sequences of F2 or S2 linkers.

The oligonucleotides were dissolved in nuclease-free water (Fresenius) to a stock concentration of 100 pmol/µl.

2.4. Yeast Two Hybrid (Y2H) Screen

For yeast two hybrid screens, genes of interest were cloned into one of two plasmids – a plasmid containing a Gal4 activation domain (G4AD) or into a plasmid containing a Gal4 DNA binding domain (G4DBD). The expressed protein fused to the G4AD is referred to as “prey”, whereas the expressed protein fused to the G4DBD is referred to as “bait”. Expressed fusion proteins were tested for possible interactions by monitoring growth on selective plates lacking histidine. If “bait” and “prey” protein are interacting the expression of the reporter gene *HIS3* is activated. For a depiction of the mechanism see Figure 7 .

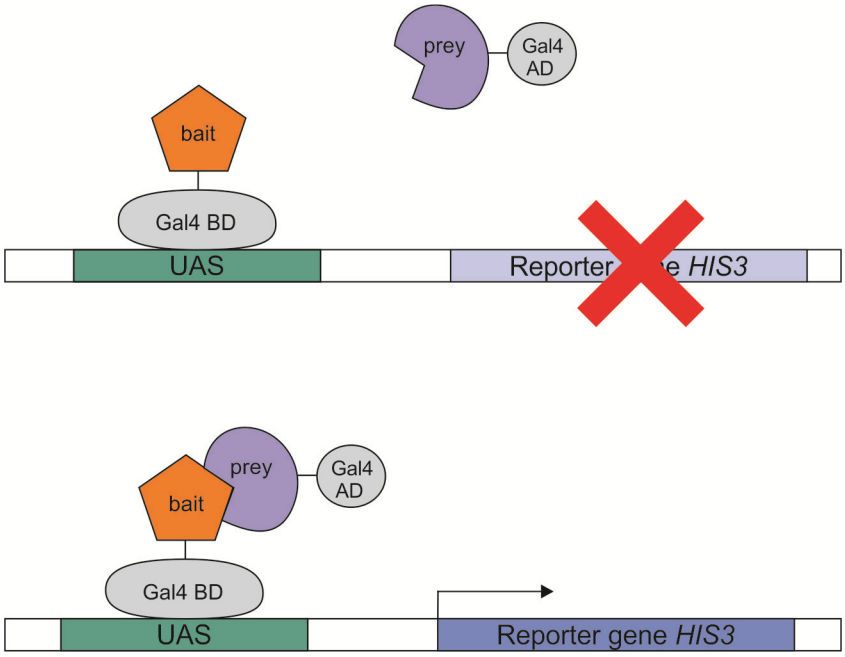

Figure 7: Depiction of Y2H mechanism. The bait protein is fused to the Gal4 DNA binding domain which is bound to an upstream activating sequence (UAS) on the DNA upstream of the *HIS3* reporter gene. The prey protein is bound to the Gal4 activation domain. Is the prey protein able to interact with the bait it brings the activation domain in close proximity of the DNA binding domain reconstituting a functional transcription activator. As a consequence the reporter gene can be expressed which allows the cells to grow on selective agar plates lacking histidine.

Genes of interest needed to be provided with restriction site recognition sequences by PCR. The PCR products as well as the plasmids were digested with appropriate restriction endonucleases, ligated and transformed into *Escherichia coli* XL-1 blue cells for amplification. G4AD- and G4DBD-plasmids were then isolated, verified by restriction analysis and sequencing and co-transformed into the Y2H reporter strain *S. cerevisiae* PJ69-4A [James, et al., 1996]. After transformation, spotting assays of strains expressing protein-1 fused to the Gal4 activation domain and protein-2 fused to the Gal4 DNA binding domain were executed.

2.4.1. PCR amplification

Polymerase chain reaction was used to add restriction sites to the genes of interest. Primers which were used for this study are listed in Table 6. Forward and reverse cloning primers contain sequences for restriction endonucleases. Genomic DNA isolated from *S. cerevisiae* W303 served as template for the PCR. Reaction setup and temperature profile are listed in Tables 7 and 8.

Table 7: PCR reaction setup to amplify cloning insert

component	volume [µl]
genomic DNA [~50 ng/µl]	1
Phusion polymerase [2 U/µl]	0.5
5x Phusion HF buffer	5
dNTPs [2 mM]	2.5
forward primer [10 pmol/µl]	2
reverse primer [10 pmol/µl]	2
nuclease-free water (Fresenius)	12
total	**25**

Table 8: Temperature profile for insert amplification

step	temperature °C	time [min]	cycles
initial denaturation	95	5	1
denaturation	95	1	
annealing	58	1	35
amplification	72	2	
final elongation	72	5-7	1
hold	4	∞	

After PCR amplification 6x loading dye was added to the product which was then separated on a 1% agarose gel (in 1xTAE buffer – see Table 9) by electrophoresis. The correct sized fragments were cut out of the gel and purified with use of the "GeneJET Gel Extraction Kit" (Thermo Fisher SCIENTIFIC®). As an alteration to the standard protocol the DNA was eluted in 25-30 µl nuclease-free water (Fresenius).

Table 9: Buffers used for gel electrophoresis

buffer	components	concentration	pH
50x TAE	tris acetate EDTA	2 M 50 mM	8.0
6x Loading dye	Tris-HCl Xylencyanol FF (BioRad) Bromphenol blue (BioRad) Glycerine EDTA	10 mM 0.03% 0.03% 60% 60 mM	7.6

2.4.2. Restriction digest

For yeast two hybrid vector construction, inserts and plasmids were cut with NEB restriction enzymes. For the complete list of restriction enzymes see Table 10. 500 ng of insert (PCR product containing restriction sites – chapter 2.4.1) and 500 ng of the plasmids pGAD-C1 and pGBDU-C1 were separately digested in a double digest reaction. For the restriction setup see Table 11. The reactions were incubated at 37°C overnight. For a double digest including *Sma*I (recommended incubation temperature at 25°C) the mix was incubated at 25°C for one hour and then shifted to 37°C.

Table 10: List of restriction enzymes used in this study

construct	vector	insert
pGBDU-C1_*MRT4*	*Bam*HI-HF, *Sal*I-HF	*Bam*HI-HF, *Sal*I-HF
pGBDU-C1_*TIF6*	*Bam*HI-HF, *Sal*I-HF	*Bam*HI-HF, *Xho*I
pGBDU-C1_*RLP24*	*Bam*HI-HF, *Sal*I-HF	*Bam*HI-HF, *Sal*I-HF
pGBDU-C1_*NOG1*	*Bam*HI-HF, *Sal*I-HF	*Bam*HI-HF, *Sal*I-HF
pGAD-C1_*UTP14*	*Sma*I, *Sal*I-HF	*Sma*I, *Xho*I
pGAD-C1_*ECM16*	*Sma*I, *Sal*I-HF	*Sma*I, *Xho*I
pGBDU-C1_*MTR4*	*Eco*RI-HF, *Sal*I-HF	*Eco*RI-HF, *Sal*I-HF
pGAD-C1_*NOP53*	*Bam*HI-HF, *Sal*I-HF	*Bam*HI-HF, *Xho*I

Enzymatic reactions were stopped by adding 6x loading dye to the suspension. The fragments were then separated on a 1% agarose gel, cut out and purified with "GeneJET Gel Extraction Kit" from Thermo Fisher SCIENTIFIC®. As an alteration to the standard protocol the DNA was eluted in 25-30 µl nuclease-free water (Fresenius).

Table 11: Restriction setup for double digest using NEB enzymes

component	volume [µl]
vector	x
insert	x
1st enzyme [20 U/µl]	0.1
2nd enzyme [20 U/µl]	0.1
10x CutSmart Buffer	2
nuclease-free water	x
total	**20**

2.4.3. Ligation

100-200 ng of purified and digested vector were mixed with a 5 fold excess of the respective insert. The ligation reactions were completed by adding 1 unit of T4 ligase (Thermo Fisher SCIENTIFIC®), 10x ligase buffer containing ATP and filled up to a total volume of 15 µl. The reaction mixture was incubated at 16°C overnight. Prior to transformation, the ligation mix was desalted by applying it on a semi permeable membrane floating on water (Millipore MF-Membrane Filters 0.025 µm VSWP) for 45 minutes at room temperature.

2.4.4. Transformation in *Escherichia coli* XL-1 blue

1 µl of the desalted ligation mix was added to 40 µl of electrocompetent *E. coli* XL-1 cells on ice. Thereafter cells were transformed by applying an electric pulse of 2500 V for 5 ms using an Eppendorf electroporator. Immediately after the pulse, 1 ml 2xTY medium was added. The cell suspension was then incubated at 37°C for 30 minutes, plated on 2xTY agar plates containing 100 µg/ml ampicillin for plasmid selection and incubated overnight at 37°C.

2.4.5. Confirmation of vector construction

To isolate and confirm the constructs, a minimum of 3 transformants of each ligation was picked from the agar plate after incubation and used to inoculate a 2 ml overnight culture in 2xTY containing 100 µg/ml ampicillin. The plasmids were isolated using the "GeneJET Plasmid Miniprep Kit" (Thermo Fisher SCIENTIFIC®). As an alteration to the standard protocol the DNA was eluted in 50 µl nuclease-free water. After the elution, about 1 µg plasmid DNA was incubated with well-chosen restriction enzymes to differentiate between empty vectors and constructs. If the restriction analysis resulted in the correct fragment sizes the constructs were sequenced by Eurofins Genomics or Microsynth.

2.4.6. Plasmid transformation of *S. cerevisiae* PJ69-4A

Yeast transformation was carried out according to basic protocol of Gietz [Gietz, 2014]. Solutions which were used for yeast transformation are listed in Table 12. Cell suspensions were inoculated to an OD_{600} of 0.1 and were grown to an OD_{600} of 0.4-0.6 in YPD media (30°C), agitated by 170 rpm. The cells were harvested by centrifugation for 6 minutes at 3500 rpm at room temperature. The cell pellet was washed twice with 10 ml of Lithium acetate (LiAc) solution at the same conditions. The pellet was then resuspended in 300-500 µl LiAc (depending on the harvested OD_{600}) and incubated at 30°C for 30 minutes (water bath). The transformation mix contained 50 µl of the competent yeast cells, 300 µl PEG

solution, 5 µl salmon sperm DNA [10 mg/ml], 500 ng of the G4AD and 500 ng of the G4DBD plasmid. The plasmids were co-transformed. The salmon sperm DNA was freshly denatured for 10 min at 95°C. The suspension was mixed and incubated for 30 min at 30°C and then heat shocked for 20 min at 42°C (water bath). The suspension was then plated on SD-Leu-Ura agar plates for plasmid selection and incubated for 2-3 days at 30°C.

Table 12: Solutions used for yeast transformation

solution	components	concentration	pH
Lithium acetate (LiAc)	lithium acetate tris-HCl EDTA	0.1 M 10 mM 1 mM	7.5
PEG solution	PEG 4000 (poly ethylene glycol) solved in LiAc	40 %	

2.4.7. Spot assay

After transformation of the Y2H reporter strain PJ69-4A with the constructed plasmids, colonies were picked to inoculate a 2 ml ONC in SD-Leu-Ura media. The cultures were adjusted to an OD_{600} of 1 and 10-fold dilutions were made in a 96-well plate from 10^0 – 10^{-3}. With a special formed metal stamp the suspensions were stamped onto SD-Leu-Ura and SD-His-Leu-Ura agar plates. SD-His-Leu-Ura plates were supplemented with different concentrations of 3-Amino-1,2,4-triazole (3-AT). The plates were incubated at 30°C up to 10 days.

2.4.8. Plasmid isolation from yeast

To verify that the Y2H strains contain the right plasmids the previously co-transformed *LEU2* and *URA3* plasmids needed to be isolated for restriction analysis. For that purpose the strains were cultivated either in SD-Leu or SD-Ura media to allow plasmid loss of one of the two plasmids. The cells were incubated

for 5 days and inoculated each day in fresh media, before they were plated on the according SD agar plates (dilutions from 10^{-4} to 10^{-6}). After two days of incubation they were replicaplated on SD agar plates to identify colonies that had lost one plasmid. The composition of amino acids for the plasmid loss experiment was different from the one used for other experiments and is listed in Table 13. 2 ml ONC of strains containing only one plasmid (either *LEU2* or *URA3*) were harvested in screw-cap tubes and resuspended in 200 µl lysis buffer (Table 14). 200 µl of glass beads as well as 200 µl of a phenol-chloroform-isoamyl alcohol mix (25:24:1) were added and the cells were disrupted by 2 minutes of high speed vortexing. After a 5 minute centrifugation step (13 000 rpm) at room temperature the aqueous phase was transferred into new Eppendorf tubes and precipitated for 10 minutes by adding 1 ml of absolute ethanol. After a 10 minute centrifugation step (13 000 rpm, 4°C) the DNA pellet was washed with 1 ml 70% ethanol (4°C) and dissolved in 10 µl nuclease-free water. The gained DNA was then retransformed in *E. coli* (chapter 2.4.4) for amplification, isolated and digested with restriction enzymes.

Table 13: Amino acid composition for yeast plasmid loss experiment

amino acid	concentration [mg/l]
adenine sulfate	10
uracil	20
L-tryptophan	50
L-histidine-HCl	20
L-arginine-HCl	50
L-methionine	20
L-tyrosine	50
L-leucine	100
L-isoleucine	50
L-lysine	50
L-phenylalanine	50
L-glutamic acid	-
L-aspartartic acid	80
L-valine	140
L-threonine	100
L-serine	-

Table 14: Lysis buffer for plasmid isolation from yeast

components	concentration	pH
Triton X-100	2%	
SDS	1%	
NaCl	100 mM	8
Tris-HCl	10 mM	
EDTA	1 mM	

2.5. Auxin inducible degradation of shuttle protein-AID fusions in a Nop58-TAP strain

The AID system is based on a unique degradation system from plants which can be transferred into other eukaryotes. By adding the natural auxin IAA (Indole-3-acetic acid) to the culture media the proteins of interest fused to the AID tag are degraded by the proteasome. For a schematic depiction of the workflow see Figure 8.

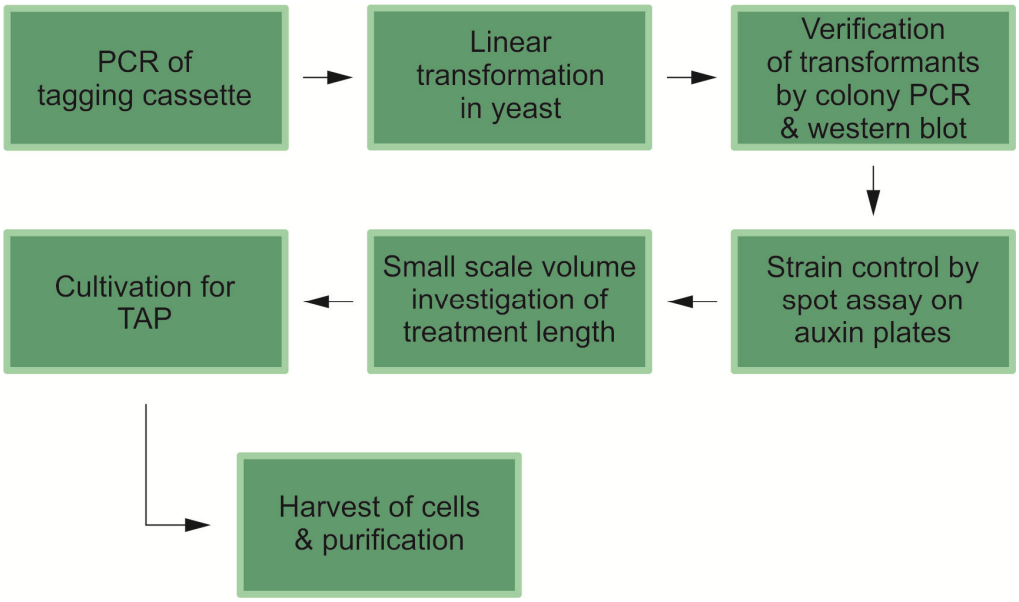

Figure 8: Workflow of auxin inducible protein degradation. After PCR amplification of tagging cassettes with Nop58 F2/S2 and Utp14 F2/S2 primers linear products were transformed into strains containing shuttle protein-AID fusions. The successful tagging was confirmed by colony PCR and western blot using protein-A antibody for Nop58-TAP and HA antibody for Utp14-HA detection. Strains were then spotted on YPD agar plates containing the auxin IAA and incubated at different temperatures. In a small volume the duration of treatment required for auxin dependent degradation for each individual strain was investigated. Finally, strains were used for tandem affinity purification (TAP) of pre-ribosomal particles using the TAP tag on Nop58.

Strains containing shuttle protein-AID fusions were kindly provided by Fasching, S. Additionally the AID tag is fused to a FLAG tag allowing the detection with anti-

FLAG antisera. In these strains as well as the original AID strain Y5159 (for genotype see Table 1) the pre-ribosome maturation factor Nop58 was provided with a TAP tag to allow tandem affinity purification of early pre-ribosomal particles. In addition Utp14 was fused with a HA tag to allow detection in western blotting. The tags were introduced by homologous recombination after linear yeast transformation (chapter 2.5.2). Transformants were screened using colony PCR (chapter 2.5.3) as well as rapid cell disruption (chapter 2.5.4) and subsequent SDS-PAGE and western blotting (chapter 2.7 & 2.9). Successfully tagged Nop58-TAP and Utp14-HA strains were tested for optimized auxin treatment conditions. Tandem affinity purification (chapter 2.6) was used to monitor possible changes in the composition of the Nop58 particle upon degradation of shuttling proteins.

2.5.1. Amplification of tagging cassettes for linear transformation of yeast

PCR was used to amplify the DNA fragments for gene tagging by homologous recombination [Longtine, et al., 1998]. The tagging cassette of plasmid pFA6a-TAP-kanMX was amplified with Nop58 specific primers containing F2/S2 linkers. The plasmid pFA6a-3xHA-natNT2 served as a template for Utp14-HA tagging and was amplified with Utp14 specific primers also containing S2/F2 linkers. Primer sequences are listed in Table 6, for PCR reaction setup and thermocycling conditions see Tables 15 & 16. When using pFA6a-3xHA-natNT2 as DNA template, DMSO was added to a final concentration of 2% to the PCR reaction setup keeping the total volume at 50 µl.

Table 15: PCR reaction setup for tagging cassette amplification

component	volume [µl]
tagging plasmid [30 ng/µl]	2.5
Phusion polymerase [2 U/µl]	1.5
5x Phusion HF buffer	10
dNTPs [2 mM]	5
tagging primer F2 [10 pmol/µl]	6.25
tagging primer S2 [10 pmol/µl]	6.25
nuclease-free water (Fresenius)	18.5
total	**50**

Table 16: Temperature profile for tagging cassette amplification

step	temperature °C	time [min]	cycles
initial denaturation	95	3	1
denaturation	95	0:50	
annealing	55	1	35
amplification	72	2:40	
final elongation	72	10	1
hold	4	∞	

2.5.2. Homologous recombination of tagging cassettes by linear transformation in yeast

Yeast transformation was performed as described in chapter 2.4.6. Since transformation rates are lower for linear DNA templates, minor alterations were made. Cells were harvested at an OD_{600} not higher than 0.4. After the washing steps the pellet was resuspended in not more than 200 µl of LiAc solution. The amount of transformed linear DNA was raised up to 15 µg per sample. The suspension needed to be mixed very carefully. After heat shock, the suspension was plated on YPD plates and replica plated the next day on YPD plates containing selection agents (30°C). After up to 4 days of incubation (depending on colony size) transformants were streaked out again on selection plates.

2.5.3. Control of correct tag integration using colony PCR

Colony PCR was used to confirm correct integration at the locus of the gene of interest after linear yeast transformation. Newly streaked out cell material from agar plates was resuspended in 20 µl of nuclease-free water. The suspension was denatured for 10 minutes at a temperature of 95°C and centrifuged for 10 minutes. 7.5 µl of the supernatant served as template DNA. Colony control primers are listed in Table 6, for reaction setup and PCR conditions see Tables 17 & 18.

Table 17: Reaction setup for colony PCR

component	volume [µl]
template DNA	7.5
Taq-Polymerase [5 U/µl]	0.5
10x ThermoPol® Reaction buffer	2.5
dNTPs [2 mM]	2
CTRL-fwd primer [10 pmol/µl]	1
Kan5b' rev primer [10 pmol/µl]	1
nuclease-free water (Fresenius)	10.5
total	**25**

Table 18: Temperature profile for colony PCR

step	temperature °C	time [min]	cycles
initial denaturation	95	5	1
denaturation	95	1	
annealing	55	1	35
amplification	72	2	
final elongation	72	5	1
hold	4	∞	

2.5.4. Rapid cell disruption

To confirm the expression of the fusion protein, a rapid cell disruption was performed. Isolated proteins were separated by SDS-PAGE and detected by western blotting. The cells were cultivated in YPD media at 30°C and an OD_{600} unit of 1 was harvested (3500 rpm, 6 minutes, room temperature). The cell pellets were resuspended in 200 µl 1.85 M NaOH including 7.5% β-mercaptoethanol and incubated on ice for 10 minutes. 200 µl of 50% TCA were added and again incubated on ice for 10 minutes. Precipitated proteins were harvested by a 15 minute centrifugation step at 13 300 rpm at 4°C. After washing the pellet twice with 1 ml of nuclease-free water at the same conditions, the proteins were dissolved in 40 µl 2.5x FSB (for the composition of FSB see Table 20). Samples were denatured for 10 minutes at 95°C and centrifuged for 10 minutes at 13 000 x g before using them for SDS-PAGE (chapter 2.7) and western blotting (chapter 2.9).

2.5.5. Determination of the optimal treatment period for the degradation of AID-fusion proteins

To find out how long it takes for the proteasome to degrade AID-fusion proteins after auxin addition to the culture a test in a small scale volume was carried out. 50 ml of YPD media were inoculated to an OD_{600} of 0.001-0.01 using an ONC. The cultures were incubated at 25°C and 170 rpm. The next day when reaching an OD_{600} of 0.8 the culture was divided into two flasks containing 20 ml of culture each. One flask was supplemented with 500 µM IAA dissolved in DMSO, the other flask serving as an untreated control was supplemented with the adequate amount of DMSO. After different treatment periods up to 2 hours, OD_{600} units of 1 were harvested. After rapid cell lysis (chapter 2.5.4), SDS-PAGE and western blotting, the AID-FLAG tag was detected with an anti-FLAG antibody.

2.6. Tandem affinity purification (TAP) of Nop58

By using the TAP protocol, protein complexes can be purified through a bait protein with a TAP tag. This tag contains a protein-A moiety, a cleavage site for TEV protease and a calmodulin binding protein. After cell lysis, TAP tag containing bait proteins together with interacting proteins bind through the protein-A moiety to IgG beads and after washing are released into the supernatant by TEV cleavage. This supernatant is called TEV eluate. With a following binding step to calmodulin beads the TEV eluate can be further purified if required.

2.6.1. Growth conditions and cell harvest

Starting from 2 liters of culture (YPD, 25°C, 110 rpm) 1 liter was harvested when reaching an OD_{600} of 1 (Beckmann Coulter ^{TM} centrifuge; 4°C, 5000 rpm, 2 min, rotor: JLA 8.1000), the remaining liter was treated with 500 µM IAA solved in DMSO. The adequate amount of DMSO was added to the untreated control. After 30 minutes of incubation the remaining liter was harvested at the same conditions. The treated cell pellets were resuspended in 10 ml double-distilled (dd). sterile water supplemented with 500 µM IAA, the untreated cell pellets were resuspended

in 10 ml of sterile water supplemented with the adequate amount of DMSO. The suspension was transferred into a 50 ml Sarstedt tube and centrifuged with the settings indicated before. The supernatant was discarded and the pellets if not processed directly frozen at -70°C.

2.6.2. Purification using the TAP protocol

Protein complexes were purified after the standard TAP protocol according to [Puig, et al., 2001; Rigaut, et al., 1999]. Buffers used for this purification are listed in Table 19. For the purification the cell pellets were thawed on ice and resuspended in 5 ml lysis buffer (LB) supplemented with: 0.5 mM PMSF; 1 mM DTT; 1x FY protease inhibitor mix by SERVA Electrophoresis GmbH. The cells were mechanically disrupted with 7.5 ml glass beads in a Merckenschlager disintegrator (B. Braun Biotech Inc., Allentown, PA, USA) for 4 minutes under CO_2 cooling. After removal of cell debris by centrifugation in an Eppendorf centrifuge (10 min, 4°C, 5000 rpm), the supernatant was transferred to centrifuge tubes and centrifuged again (Beckmann Coulter ^{TM} centrifuge; 10 min, 4°C, 18500 rpm, rotor: JA25.50). Another centrifuge step followed at the same conditions for 30 minutes to completely remove cell debris. A 40 µl aliquot of the supernatant (= crude extract) was frozen away. The rest of the supernatant of each sample was then incubated with 150 µl settled IgG-sepharose beads (GE Healthcare). To bind proteins to the IgG beads the suspension was incubated for 90 minutes under constant rotaion at 4°C. Then the suspension was centrifuged (5min, 3000 rpm, 4°C) and the IgG beads were washed (Sarstedt tubes) one time with 6 ml LB (supplemented with 1 mM DTT) and three times with 1 ml cleavage buffer (CB) supplemented with 0.5 mM DTT to remove unbound proteins. All washing steps were carried out at 3000 rpm, 4°C for 3 minutes. After washing the beads, 500 µl CB (supplemented with 0.5 mM DTT) were added and transferred into a 0.5 ml PCR tube. 120 µl were taken away, centrifuged to remove the washing buffer completely (2 min, 3000 rpm, 4°C) and the IgG beads were frozen at -70°C for further RNA isolation. The remaining beads were centrifuged with the same settings to remove the buffer. Each sample was then resuspended in 62.5 µl TEV

mix (consisting of 60 µl CB, 0.5 mM DTT, 2.5 µl TEV protease) and incubated for 60 minutes under constant rotation at room temperature to cleave off the protein-A moiety from the TAP tag and therefore eluting the protein complexes. Afterwards the samples were centrifuged three times (5000 rpm, 3 min, 4°C) to remove all IgG beads. The supernatant (= TEV eluate) was stored at -20°C.

Gained samples were prepared as followed:

- 10 µl crude extract + 90 µl 2x FSB
- 30 µl TEV eluate + 20 µl of 5x FSB

Samples were used for SDS-PAGE (chapter 2.7), subsequent colloidal blue staining (chapter 2.8) and western blotting (chapter 2.9).

Table 19: Buffers used for tandem affinity purification

buffers	components	concentrations	pH
lysis buffer (LB)	HEPES/KOH	20 mM	7.5
	KCl	10 mM	
	$MgCl_2$	2.5 mM	
	EGTA	1 mM	
cleavage buffer (CB)	HEPES/KOH	20 mM	7.5
	KCl	10 mM	
	MgCl2	2.5 mM	
	EGTA	1 mM	
	NaCl	100 mM	

2.7. SDS-PAGE

Bis-Tris 12% gels by NuPAGE® Novex® were used for protein samples gained from the test degradation (chapter 2.5.5). Bis-Tris 4-12% gradient gels were used for protein separation after tandem affinity purification. Electrophoresis of NuPAGE® Novex® gels was carried out in a XCell SureLock™ Mini-Cell Electrophoresis System (Thermo Fisher SCIENTIFIC®) containing MOPS buffer (Life Technologies). Proteins were separated by applying a voltage of 100-140V. Buffers used for SDS-PAGE are listed in Table 20.

Table 20: Buffers used for SDS-PAGE

buffers	components	concentration	pH
MOPS running buffer	MOPS tris base SDS EDTA	50 mM 50 mM 0.1% 1 mM	7.7
5x FSB (final sample buffer)	tris-HCl SDS DTT glycerol bromophenol blue	312.5 mM 10% 600 mM 40% 0.02%	6.8

2.8. Colloidal blue staining

This method was used after tandem affinity purification to stain Bis-Tris gels to make protein bands visible. The Colloidal Blue Staining Kit from Thermo Fischer SCIENTIFIC® was used.

2.9. Western Blot

Proteins were transferred from SDS gels onto a PVDF (polyvinylidene difluoride) membrane (Millipore) using a tank-blot-system (BIO-RAD) containing CAPS buffer. By using an electric current (220 mA, 90 minutes) proteins were transferred onto the membrane. The membrane was blocked (to prevent non-specific binding) at 4°C overnight with 0.5% dry milk powder dissolved in 1xTST buffer. For the list of buffers see Table 21. The membrane was then incubated for 1 hour with primary antibodies directed against the protein of interest. The membrane was washed 3 times with 1xTST buffer for 5 minutes and incubated with the secondary antibody directed against rabbit IgG. When using the conjugated HA- and Flag-antibodies the membrane can be detected after one hour of incubation without the need of a secondary antibody. For a complete list of antibodies see Table 22. After incubation with the secondary antibody the membrane was washed as described above. All incubation and washing steps were performed at room temperature under gentle agitation. After the washing steps the membrane was incubated for 3 minutes with 1 ml of Clarity™ ECL agent (BIO-RAD) and detected by ChemiDoc™ BIO-RAD using the chemiluminescence detection program. After

detection the membrane was incubated with stripping buffer for 20 minutes at 60°C to remove bound antibodies. The membrane was washed 4 times for 10 minutes.

Table 21: Buffers used for western blotting

Buffers	Components	Concentration	pH
CAPS transfer buffer	CAPS Methanol	10 mM 10%	11.0
1x TST buffer	Tris-HCl NaCl Tween20	50 mM 150 mM 0.1%	7.4
Stripping buffer	Tris-HCl β-mercaptoethanol SDS	60 mM 100 mM 2%	6.8

Table 22: Antisera used in this study.
All antisera were diluted in 1% milk powder in 1x TST buffer.

antibody	source	dilution	host
CBP	Sigma Aldrich	1:5000	rabbit
Noc1	University of Regensburg	1:5000	rabbit
Noc2	University of Regensburg	1:5000	rabbit
Rcl1	A. Henras	1:5000	rabbit
Sof1	E. Hurt	1:600	rabbit
Rrp12	M. Dosil	1:5000	rabbit
Rok1	K. Karbstein	1:5000	rabbit
HA (conjugated)	Roche	1:10000	rat
Flag (conjugated)	Sigma Aldrich	1:10000	mouse
Nop RP1-4	E. Hurt	1:7500	rabbit
Rpa135	M. Oaks	1:3000	rabbit
RpL16	S. Rospert	1:40000	rabbit
GAPDH	G. Daum	1:40000	rabbit
Protein A	Sigma Aldrich	1:10000	rabbit
anti rabbit IgG	Sigma Aldrich	1:15000	goat

3. Results

3.1. Auxin dependent degradation of shuttling proteins

3.1.1. Growth analysis of generated strains on auxin containing agar plates

After tagging of Nop58-TAP and Utp14-HA in strains expressing shuttling protein-AID fusions, the cells were spotted on YPD agar plates supplemented with 500 µM auxin (IAA) to analyse possible growth defects due to auxin induced degradation of shuttling proteins. The concentration of 500 µM was chosen according to the findings described in [Nishimura, et al., 2009]. After diluting an ONC to an OD_{600} of 1, 10-fold dilutions up to 10^{-3} were made in sterile 96-well plates. The suspensions were stamped on agar plates and incubated at two temperatures: 30°C and 25°C (Figure 9).

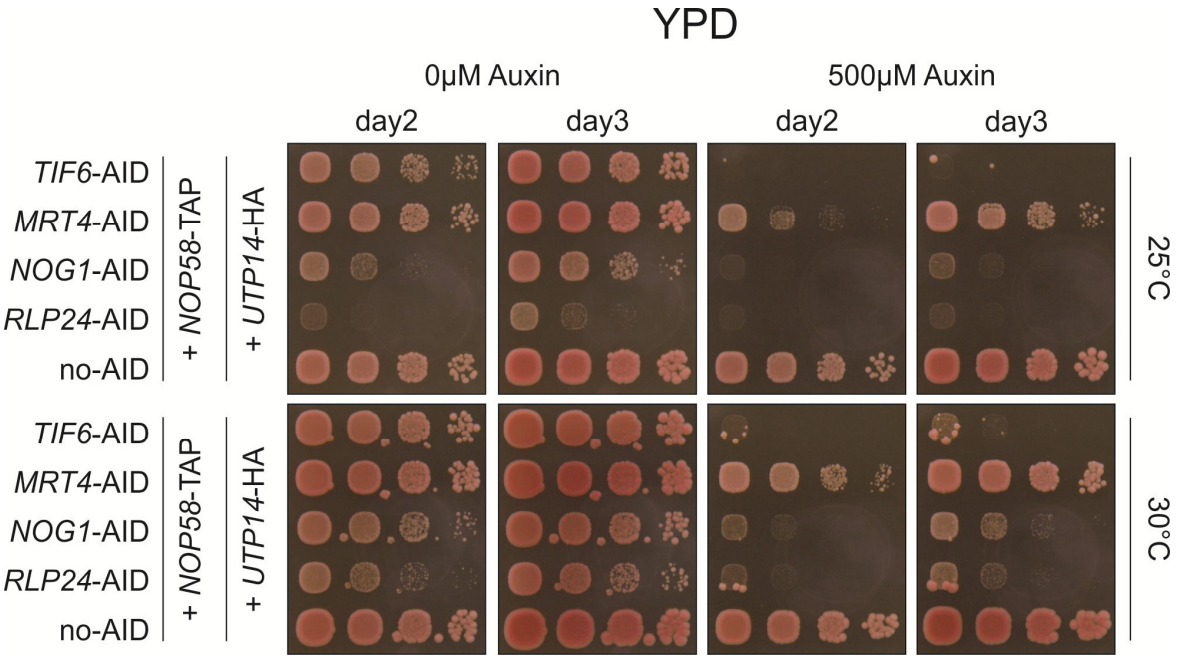

Figure 9: Dot spot of strains expressing AID-fusion tagged shuttling proteins on auxin plates. 10^{0}-10^{-3} dilutions of an OD_{600} of 1 were prepared for each strain in sterile 96-well plates and spotted on YPD without or with 500 µM auxin IAA (Indole-3-acetic acid) and incubated at 25°C and 30°C. The parent strain Y5159 (no-AID) served as a control. Shuttling proteins (*TIF6*, *MRT4*, *NOG1*, and *RLP24)* were provided with an AID tag. In all of these strains *NOP58* was tagged with a TAP tag and *UTP14* with a HA tag.

Figure 9 shows the growth behaviour of strains expressing shuttling proteins fused with an AID-fusion tag in the presence or absence of auxin. The control strain (no-AID) showed no difference in growth on the YPD plates containing 500 µM auxin in comparison to the control plate without the compound. At 25°C all strains expressing the shuttling protein-AID tag fusion protein showed a growth defect on auxin plates. The strain carrying the Mrt4-AID fusion was still viable on auxin plates but shows reduced growth. The *NOG1*-AID strain already showed reduced growth on the plates without auxin, as well as *RLP24*-AID which grew very slowly.

At 30°C all strains showed better growth than on 25°C. Thus, the degradation seems to be more effective at 25°C than at 30°C. This observation is consistent with literature [Nishimura, et al., 2009].

3.1.2. Kinetics of AID-fusion protein degradation

To identify the optimal incubation time for auxin induced degradation of the AID-fusion proteins a test degradation in a small scale volume was carried out. 50 ml of culture were incubated at 25°C to an OD_{600} of 1. The culture was then split up in 20 ml of untreated and 20 ml of treated culture. After different treatment periods an OD_{600} unit of 1 was harvested and the degradation of the tagged proteins was tracked by a western blot analysis (chapter 2.9) and detection of the Flag tag which is part of the AID tag. In Figure 10A the degradation of the Tif6-AID fusion protein is shown. Compared to the untreated controls the samples containing auxin showed a rapid decrease in band intensity already after 15 minutes of incubation time. The signals of GAPDH and RpL16 were nearly the same in all samples indicating that the same amount of protein was loaded onto the gel before blotting. Figure 10B shows the degradation of the Mrt4-AID fusion protein detected by anti-Flag antibody. The bands of the treated samples also diminished very fast within 15-30 minutes.

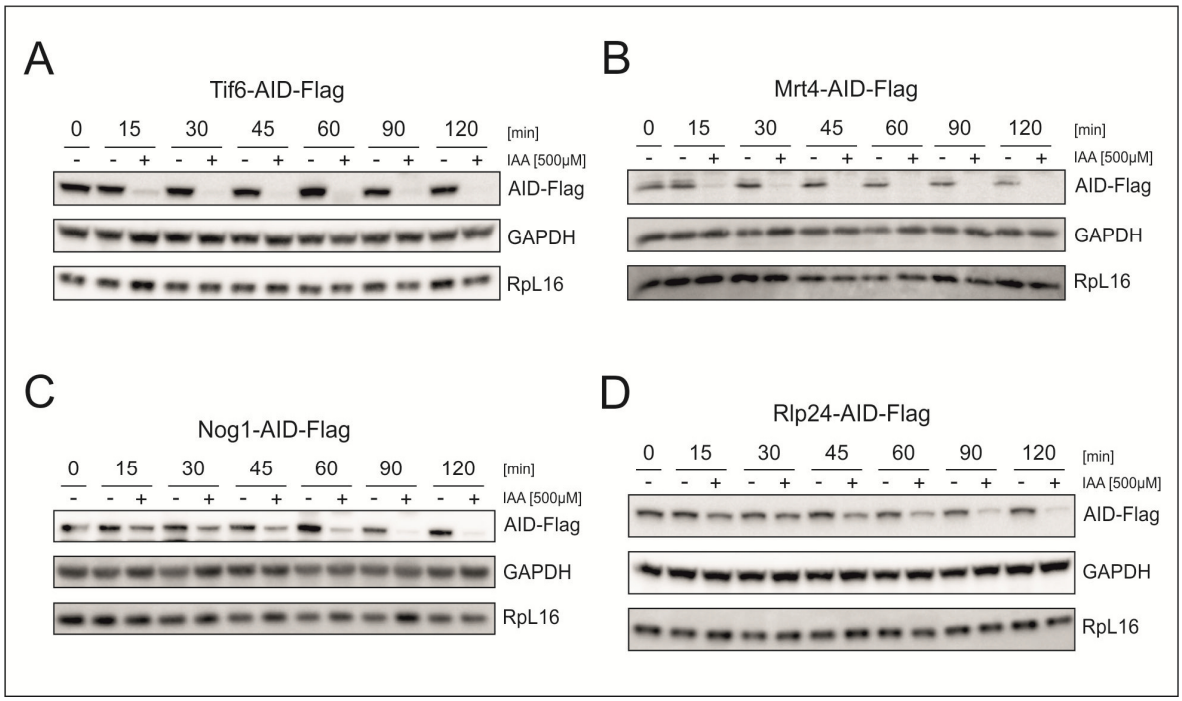

Figure 10: Timeline of auxin induced degradation of AID fusion proteins. Western blots of strains expressing AID-fusion proteins, incubated with 500 µM auxin (IAA) over 2 hours. All shown strains also express Nop58-TAP and Utp14-HA. Treated (+) samples were compared to untreated (-) samples. The degradation of the AID-fusion protein was detected by an antibody directed against the Flag tag. As a loading control membranes were also incubated with antibodies directed against GAPDH and ribosomal protein L16 (RpL16).

Figure 10C shows the degradation of Nog1-AID. The band intensity of the treated samples compared to the untreated controls was weaker after 15 minutes of treatment. But looking at the loading controls GAPDH and RpL16 the bands were a little more intense in the treated samples. Probably more protein was loaded in the treated samples. The band for the Nog1-AID protein was completely abolished after 90 minutes. As for Rlp24-AID shown in Figure 10D the band in the treated samples was still detectable after 45 minutes of treatment. After 90 minutes the band was nearly vanished. Taken together, the results show that Tif6- and Mrt4-AID proteins are degraded within 15 minutes, while about half of the Nog1- and Rlp24-AID proteins are degraded within 30 minutes of auxin treatment.

Based on these experiments, a treatment period of 30 minutes was applied for subsequent tandem affinity purification.

3.1.3. Tandem affinity purification of Nop58 upon degradation of shuttling proteins

To monitor possible changes in particle composition upon degradation of single shuttling proteins, early pre-ribosomal particles were purified using TAP fusions with Nop58, a component of the U3 snoRNP, as bait protein. The composition of the particles was analysed by SDS-PAGE (chapter 2.7) and western blotting. Untreated samples were compared to cells which were treated with 500 µM auxin (IAA) for 30 minutes at 25°C before being harvested for the purification. The results of this experiment are shown in Figure 11.

In Figure 11A, the SDS-gel stained with colloidal blue after separating the proteins by electrophoresis is shown. The sample volume of this gel was adjusted to the amount of bait protein by detecting it with an antibody directed against the calmodulin binding protein (cbp) in a prior western blot (data not shown). Although the loaded samples were adjusted in Figure 11 the amount of bait protein the TEV-eluate lanes containing samples of the strain expressing the Rlp24-AID-Flag fusion showed weaker band intensity than the other samples. Slight changes in band intensity and particle composition between treated and untreated samples could be observed as well as slight differences between the different strains. For example the two marked bands in the untreated Nog1-AID sample differed from the other samples. The band at about 120 kDa might be Nog1-AID. The assignment of single bands to certain proteins has to be done by mass spectrometry. The strong band at 55 kDa in the untreated Mrt4-AID sample is not present in the sample of the treated cells and only weakly present in the Tif6 samples. This band likely represents the IgG heavy chain and signals contamination of the sample with IgG beads.

In Figure 11B the western blot of the purification is shown. The bait protein Nop58 was detected with an antibody against the calmodulin binding protein which is still fused to the bait protein after TEV-cleavage. The amounts of the bait protein were well adjusted. The membrane was incubated with a few antibodies directed against 90S factors as well as early pre-60S factors. Since the strains express

AID-Flag tagged forms of different shuttling proteins the degradation of these fusion proteins was analysed by detecting the Flag tag. In the long exposure of the Flag tag western blot it is obvious that the Tif6-AID fusion (~51 kDa) as well as the Mrt4-AID (~52 kDa) fusion were completely gone after the 30 minute treatment period.

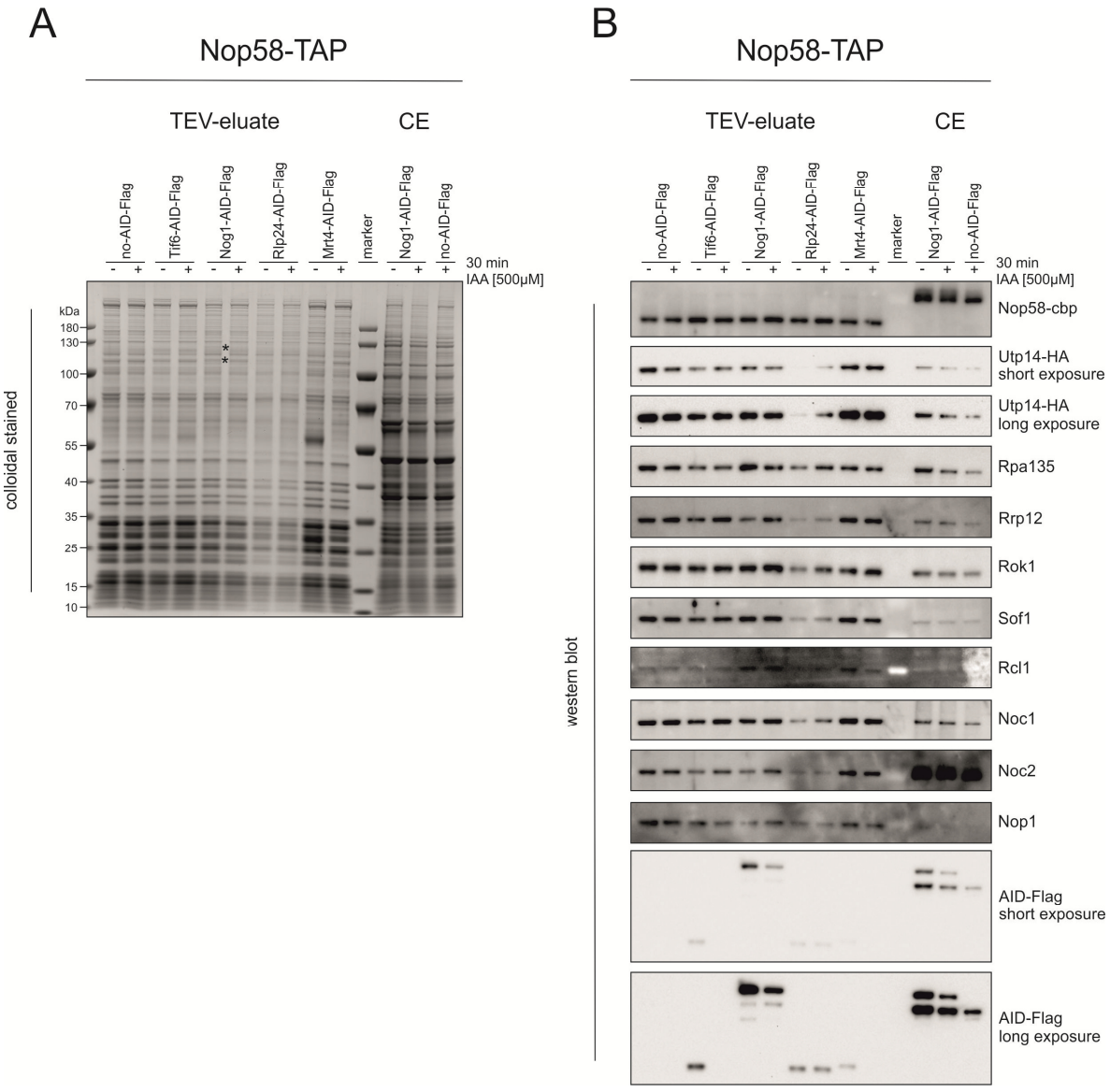

Figure 11: SDS-gel and western blot after Nop58 tandem affinity purification. A Crude extracts (CE) and TEV-eluates of the strains expressing different AID fusion proteins were separated by a 4-12% polyacrylamid gradient gel and colloidal blue stained. The marker used was the Pageruler Prestained Protein ladder, Thermo scientific. The untreated (-) samples were compared to treated (+) samples which were incubated with 500 µM auxin (IAA) for 30 minutes before harvest. * - marked bands which were slightly different than in other samples. In **B** the western blot after SDS-PAGE is shown. Different antibodies directed against 90S and early 60S factors were used to detect the protein components of the purified complex. Utp14 was detected with an antibody directed against the HA. The efficiency of auxin induced degradation of the AID-Flag tagged proteins was examined by incubation with an antibody directed against the Flag tag. The bait protein Nop58 was detected with an antibody directed against the calmodulin binding protein (cbp).

In addition, Nog1-AID (~100 kDa) was strongly reduced in the auxin treated sample, while the signal for Rlp24-AID (~50 kDa) was only slightly reduced. However, the overall yield of the co-purifying proteins in the strain expressing the Rlp24-AID fusion was strongly reduced.

This finding suggests that the AID tag on Rlp24 interferes with loading of Nop58-TAP and hence U3 snoRNP onto early pre-ribosomal particles. The samples of Tif6-AID and Nog1-AID expressing strains showed a reduction of Utp14 independent of the auxin treatment compared to the control. In the Noc1 western blot a decrease of band intensity in the untreated Tif6-AID and Nog1-AID samples compared to the control could be observed but seemed to increase upon degradation of the AID tag. A similar picture was observed for Noc2 and Rrp12, although these proteins associate at a later stage with the pre-ribosome [Chaker-Margot, et al., 2015]. The amount of Rpa135 seemed to be decreased in the Tif6-AID expressing strains in the untreated as well as in the treated samples. In contrast, the amount of Rpa135 increased in the untreated Nog1-AID sample. Differences in band intensity in the Rcl1 western blot are likely due to detection problems.

The C-terminal AID tag is obviously interfering with an early maturation step enforcing the assumption that Tif6, Nog1 as well as Rlp24 are required for this early processes.

3.2. Yeast two hybrid interaction studies

The yeast two hybrid (Y2H) method is based on the reconstitution of a functional Gal4 transcription activator. To generate Y2H strains one plasmid expressing a Gal4 activation domain fused to a so-called “prey” protein is co-transformed into a reporter strain with a second plasmid expressing a Gal4 DNA binding domain fused to a so-called “bait” protein. If the expressed fusion proteins are interacting with each other *in vivo*, the Gal4 activation (G4AD) comes in close proximity to the Gal4 DNA binding (G4DBD) domain which forms a functional transcription

activator. As a consequence the expression of the *HIS3* reporter gene is activated allowing the cells to grow on agar plates lacking histidine. To investigate possible interactions between early pre-ribosome maturation factors and shuttling proteins, *TIF6*, *MRT4*, *NOG1* and *RLP24* were cloned into the G4DBD vector and *UTP14* and *ECM16* were cloned into the G4AD vector. Strains carrying a G4DBD vector containing an individual shuttling protein and the G4AD vector containing one of the 90S factors were tested for activation of the reporter gene by monitoring the growth on selective plates lacking histidine.

The cells were spotted in 10-fold dilutions up to 10^{-3} on SD-Leu-Ura plates for plasmid maintenance. The G4AD plasmid pGAD-C1 contains a *LEU2* marker and the G4DBD plasmid pGBDU-C1 contains the *URA3* marker. By spotting on SD-Leu-Ura-His plates, only cells in which the two expressed fusion proteins interact with each other are able to grow. SD-Leu-Ura-His plates were additionally supplemented with different concentrations of 3-amino-1,2,4-triazole which acts as a competitive inhibitor to the *HIS3* gene product imidazoleglycerol-phosphate dehydratase.

In Figure 12 a dot spot of the interaction screen between Utp14 and shuttling proteins is shown. Different strains containing G4AD and G4DBD plasmids were spotted on selection plates. The actual tested interactions of Utp14 with individual shuttling proteins are marked with an arrow. Below each investigated interaction a control strain containing the G4DBD with the shuttling protein fusion and the empty G4AD vector was spotted. Plasmids containing the published interaction partners Nop53 and Mtr4 [Thoms, et al., 2015] served as a positive control. Only the strain containing Rlp24 and Utp14 shows growth on the plates lacking histidine.

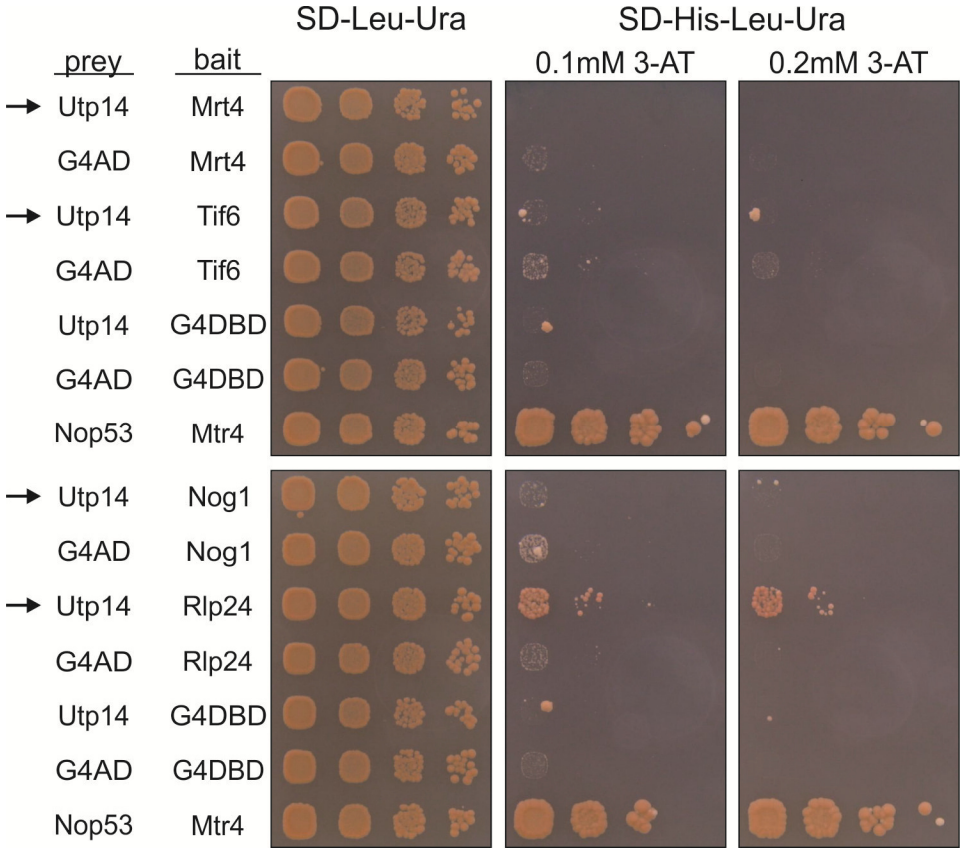

Figure 12: Yeast two hybrid assay testing for interaction between Utp14 and shuttle proteins. Plasmids expressing different shuttling proteins fused to the Gal4 DNA binding domain (bait) and Utp14 fused to the Gal4 activation domain (prey) were co-transformed in the Y2H reporter strain *S. cerevisiae* PJ69-4A. Cell suspensions with an OD_{600} of 1 were spotted in dilutions from 10^{0} to 10^{-3} onto SD-Leu-Ura and SD-Leu-Ura-His plates supplemented with 0.1 and 0.2 mM 3-AT. SD-Leu-Ura plates were incubated at 30°C for 3 days, while the SD-Leu-Ura-His plates were incubated for 10 days. Tested interactions are marked with an arrow, the others are controls. The published interaction partners Nop53 and Mtr4 served as a positive control [Thoms, et all., 2015].

To reproduce these findings another set of 6 newly transformed strains containing the G4AD-Utp14 and G4DBD-Rlp24 fusion was spotted in Figure 13.

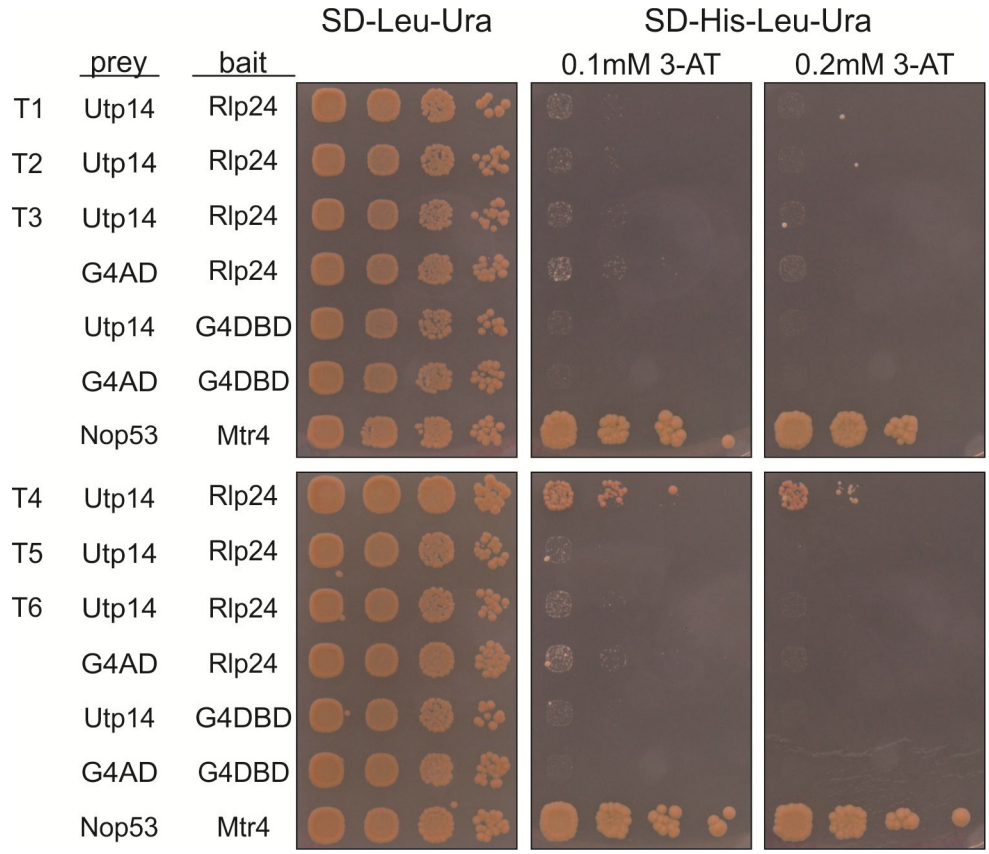

Figure 13: Yeast two hybrid assay testing for interaction between Utp14 and Rlp24. Plasmids expressing Rlp24 fused to the Gal4 DNA binding domain (bait) and Utp14 fused to the Gal4 activation domain (prey) were co-transformed in the Y2H reporter strain *S. cerevisiae* PJ69-4A. 6 transformants (T1-T6) were spotted in dilutions from 10^0 to 10^{-3} based on an OD_{600} of 1 onto SD-Leu-Ura and SD-Leu-Ura-His plates supplemented with 0.1 and 0.2 mM 3-AT. SD-Leu-Ura plates were incubated at 30°C for 3 days, while the SD-Leu-Ura-His plates were incubated for 10 days. The published interaction partners Nop53 and Mtr4 served as a positive control [Thoms, et all., 2015].

Against the expectations only one of the transformants (T4) showed growth on SD-Leu-Ura-His plates supplemented with 3-AT.

The interaction screen between Ecm16 and shuttling proteins is shown in Figure 14. Different strains containing Ecm16 in G4AD and various shuttling proteins in G4DBD plasmids were spotted on selection plates. The tested interactions are marked with an arrow. Below each investigated interaction a control strain containing the G4DBD shuttling protein fusion and the empty G4AD vector were spotted. The positive control was the same as in Figure 12. Only the strain expressing Tif6-bait and Ecm16-prey was able to grow on SD-Leu-Ura plates lacking histidine. The plates were supplemented with 0.2 mM 3-AT.

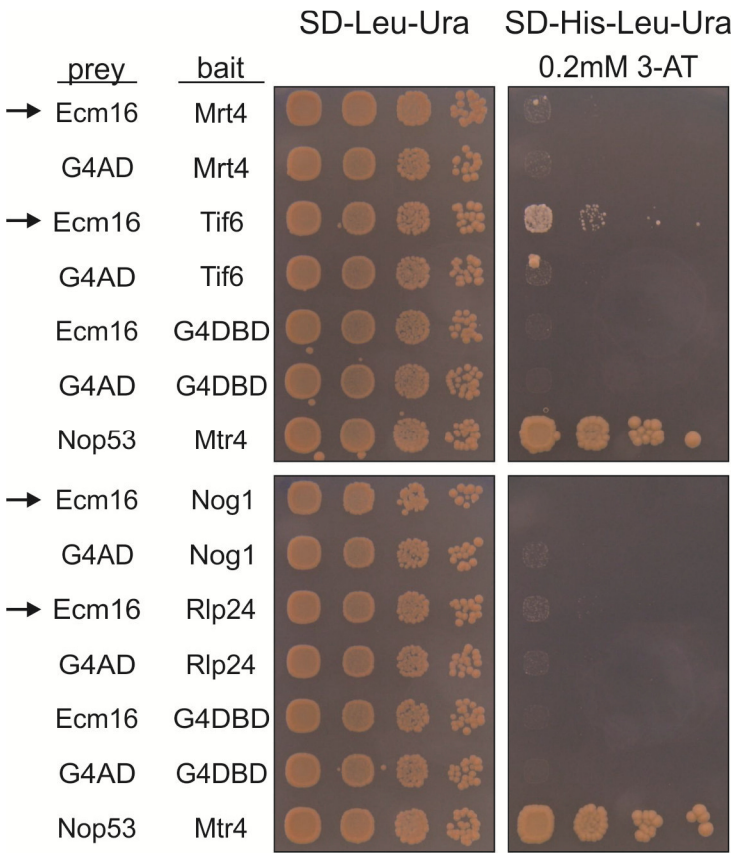

Figure 14: Yeast two hybrid assay testing for interaction between Ecm16 and shuttle proteins. Plasmids expressing different shuttling proteins fused to the Gal4 DNA binding domain (bait) and Ecm16 fused to the Gal4 activation domain (prey) were co-transformed in the Y2H reporter strain *S. cerevisiae* PJ69-4A. The cell suspensions with an OD_{600} of 1 were spotted in dilutions from 10^{0} to 10^{-3} onto SD-Leu-Ura and SD-Leu-Ura-His plates supplemented with 0.2 mM 3-AT. SD-Leu-Ura plates were incubated at 30°C for 3 days, while the SD-Leu-Ura-His plates were incubated for 10 days. Tested interactions are marked with an arrow, the others are controls. The published interaction partners Nop53 and Mtr4 served as a positive control [Thoms, et all., 2015].

To reproduce these findings another set of 6 newly transformed strains containing the G4AD-Ecm16 and G4DBD-Tif6 fusion proteins were investigated by spotting assays as shown in Figure 15.

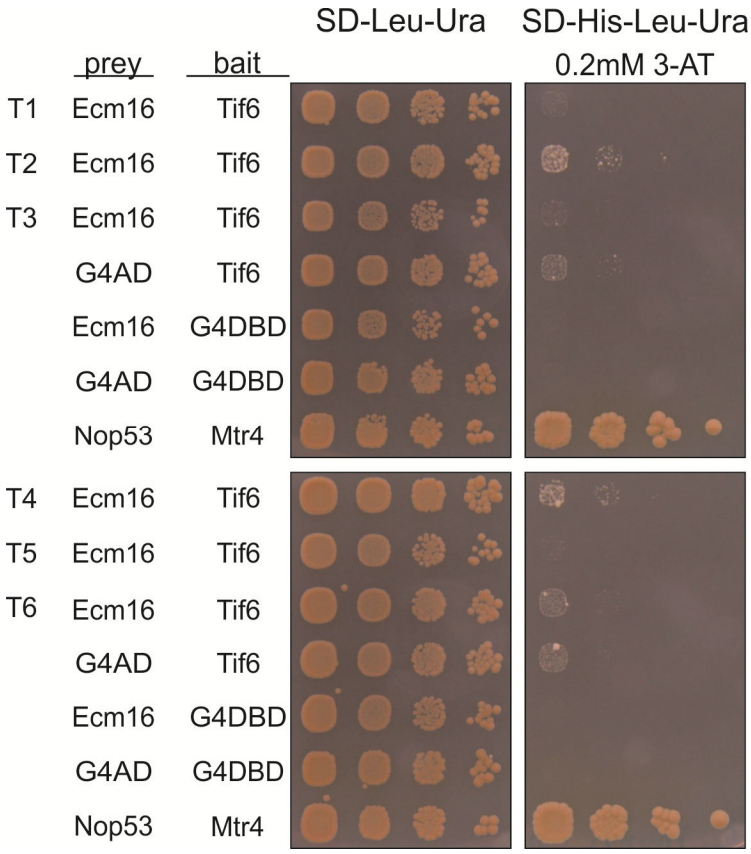

Figure 15: Yeast two hybrid assay testing for interaction between Ecm16 and Tif6. Plasmids expressing Tif6 fused to the Gal4 DNA binding domain (bait) and Ecm16 fused to the Gal4 activation domain (prey) were co-transformend in the Y2H reporter strain *S. cerevisiae* PJ69-4A. 6 transformants (T1-T6) were spotted in dilutions from 10^{0} to 10^{-3} based on an OD_{600} unit of 1 onto SD-Leu-Ura and SD-Leu-Ura-His plates supplemented with 0.2 mM 3-AT. SD-Leu-Ura plates were incubated at 30°C for 3 days, while the SD-Leu-Ura-His plates were incubated for 10 days. The published interaction partners Nop53 and Mtr4 served as a positive control [Thoms, et all., 2015].

Only two of the newly transformed strains showed a stronger growth than the control strain expressing the Tif6-bait protein from pGBDU and containing the pGAD vector control without Ecm16.

3.3. Attempts to investigate the different behaviour of transformants in Y2H assays

To investigate why not all six transformants of the experiments in figures Figure 13 & Figure 15 showed the same phenotype in the spotting assay, the sequences of the transformed plasmids were checked again to rule out a frameshift mutation of the constructed plasmids. In addition, the plasmids were isolated from chosen strains showing interaction and transactivation as determined by growth on histidine lacking media as well as plasmids from selected transformants showing no transactivation.

These plasmids were subjected to restriction analysis with chosen enzymes to differentiate empty vectors from those actually containing the cloned genes.

3.3.1. Sequence analysis of Y2H plasmids

The generated plasmids were sequenced by either Microsynth or Eurofins Genomics. In addition, the cloning of *UTP14* and *ECM16* in G4AD as well as the cloning of *RLP24* and *TIF6* in G4DBD was *in silico* modelled using the program Serial Cloner (version 2.6; Serialbasics). The analysed sequence was aligned with the one predicted in Serial Cloner.

Figure 16 is a schematic representation of the G4AD-*UTP14* fusion. In Figure 16A a sector of the sequence of G4AD-*UTP14* representing the fusion site between the N-terminal *GAL4* activation domain and the C-terminal *UTP14* is shown. Above and below the nucleotide sequence the amino acid sequence is depicted. The sequence of the constructed plasmid was identical to the *in silico* predicted one. In Figure 16B the area between the C-terminus of *UTP14* and the N-terminus of the *GAL4* terminator sequence (transcription stop of the mRNA) is shown.

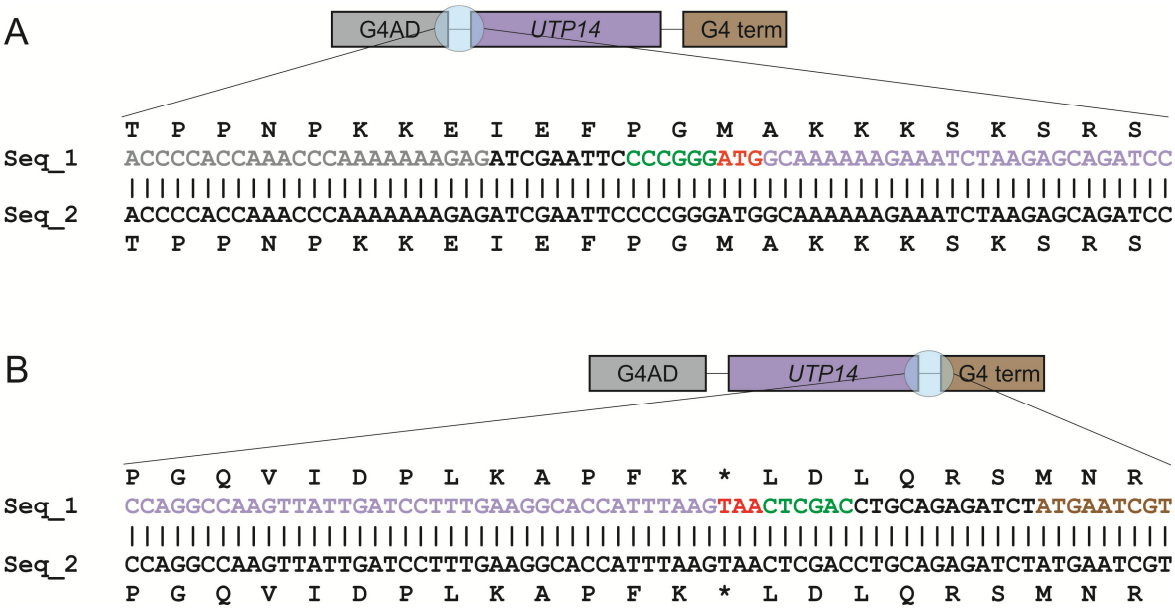

Figure 16: Sequence analysis of the generated G4AD-*UTP14* vector. A shows an excerpt of the ligated area between the G4AD sequence and *UTP14*, while in **B** the area between *UTP14* and the Gal4 terminator is depicted. Seq_1 represents a theoretical sequence, while Seq_2 shows the experimentally determined sequence. *UTP14* is coloured in purple, the G4AD in grey, the Gal4 terminator in brown, start/stop codons are coloured in red, the nucleotides derived from the restriction site sequences are shown in green. Above Seq_1 and below Seq_2 the amino acid sequence is shown, stop codon is depicted with a star.

In course of PCR amplification an *Xho*I site was introduced at the 3' end of the *UTP14* gene. After cleavage, the PCR product was ligated into *Sal*I cleaved vector. These enzymes generate overlapping overhangs which allow ligation. After the ligation of vector and insert the gained sequence was a mix of these two recognition sites no longer being able to be cleaved with either of the two enzymes.

The sequence of the G4DBD-*RLP24* vector is shown in Figure 17. Figure 17A depicts the area between the C-terminal end of the DNA binding domain and the N-terminus of *RLP24*. Above and below the nucleotide sequence, the amino acid sequence is depicted. The sequence of the constructed plasmid was identical to the *in silico* predicted one. In Figure 17B the area between the C-terminus of *RLP24* and the N-terminus of the Gal4 terminator sequence is shown. The sequences were again identical.

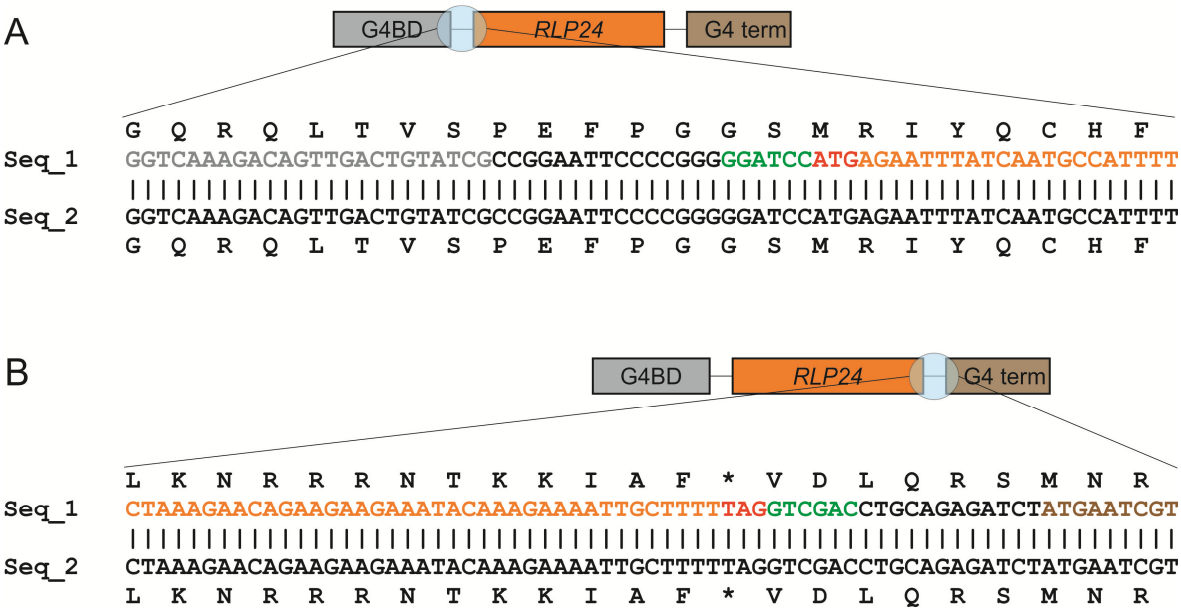

Figure 17: Sequence analysis of the generated G4DBD-*RLP24* vector: A shows an excerpt of the ligated area between the G4BD sequence and *RLP24*, while in **B** the area between *RLP24* and the Gal4 terminator is depicted. Seq_1 represents a theoretical sequence, while Seq_2 shows the experimentally determined sequence. *RLP24* is coloured in orange, the G4BD in grey, the Gal4 terminator in brown, start/stop codons are coloured in red, the nucleotides derived from the restriction site sequences are shown in green. Above Seq_1 and below Seq_2 the amino acid sequence is shown, stop codon is depicted with a star.

Exactly the same sequence analyses were carried out for the investigated interaction partners G4AD-*ECM16* and G4DBD-*TIF6* and are shown in Figure 18Figure 19. The experimentally determined sequences were again identical to the *in silico* predicted ones without any indication for deletions or mismatches.

Apart of the ligated areas also the whole genes were sequenced (data not shown) showing 100% sequence identity to the templates. The results showed no indication of mutations introduced during PCR amplification or cloning of the genes of interest into Gal4 activation and Gal4 DNA binding domain containing vectors.

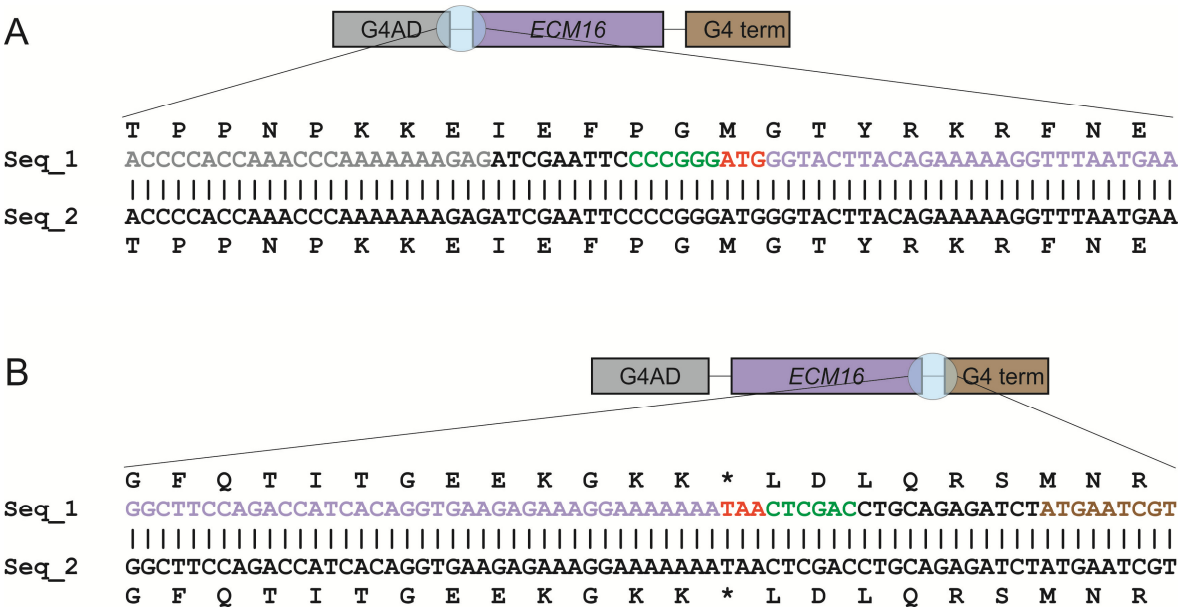

Figure 18: Sequence analysis of the generated G4AD-*ECM16* vector. A shows an excerpt of the ligated area between the G4AD sequence and *ECM16*, while in **B** the area between *ECM16* and the Gal4 terminator is depicted. Seq_1 represents a theoretical sequence, while Seq_2 shows the experimentally determined sequence. *ECM16* is coloured in purple, the G4AD in grey, the Gal4 terminator in brown, start/stop codons are coloured in red, the nucleotides derived from the restriction site sequences are shown in green. Above Seq_1 and below Seq_2 the amino acid sequence is shown, stop codon is depicted with a star.

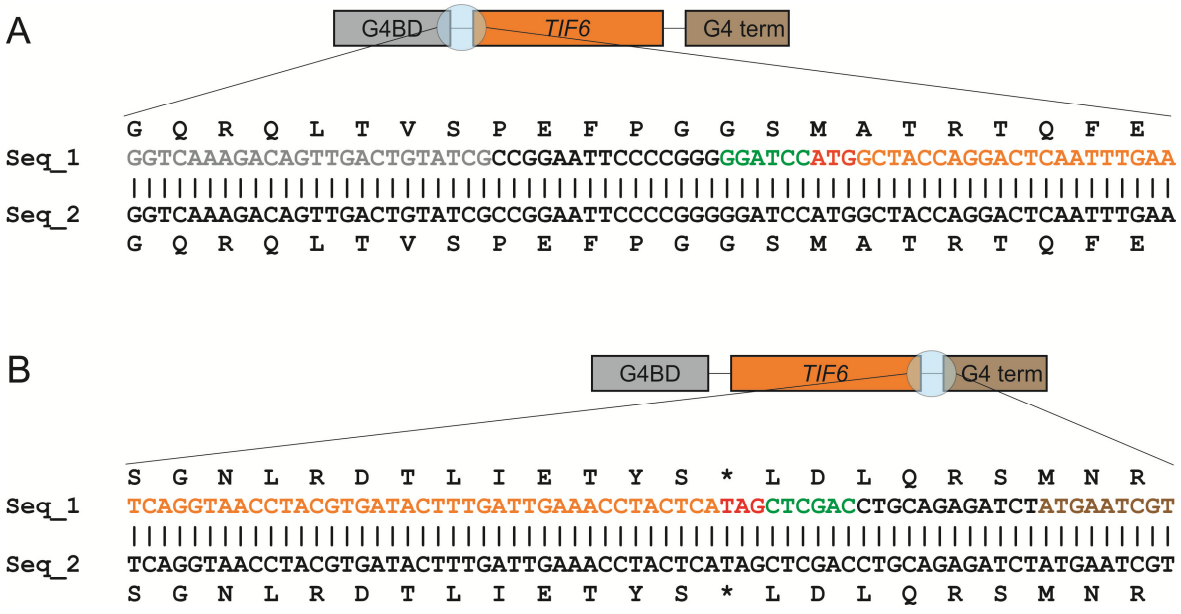

Figure 19: Sequence analysis of the generated G4DBD-*TIF6* vector: In **A** an extract of the ligated area between the G4BD sequence and *TIF6* is shown, while **B** depicts the area between *TIF6* and the Gal4 terminator sequence. Seq_1 represents a theoretical sequence, while Seq_2 shows the sequence experimentally determined sequence. *TIF6* is coloured in orange, the G4BD in grey, the Gal4 terminator in brown, start/stop codons are coloured in red, the nucleotides derived from the restriction site sequences are shown in green. Above Seq_1 and below Seq_2 the amino acid sequence is shown, stop codon is depicted with a star.

3.3.2. Restriction analysis of isolated Y2H plasmids

For investigation of the possible interaction partners G4AD-Utp14 & G4DBD-Rlp24, transformants number T4, T5 and T6 of the dot spot assay in Figure 13 as well as the original transformant shown in Figure 12 (referred to as T0 from now on) and controls K1 and K2 were used. The strain G4AD-Utp14 & G4DBD is referred to as K1; the strain G4AD & G4DBD-Rlp24 is referred to as K2.
The strains contain one plasmid with *LEU2* and another plasmid with an *URA3* marker. Therefore both SD-Leu and SD-Ura media were inoculated with the chosen yeast strains and incubated as described in the material and methods section (for plasmid loss and isolation see chapter 2.4.8). The cells were harvested and the plasmids were isolated, retransformed into *E. coli* for amplification, isolated from bacteria and a restriction analysis was carried out.

G4AD derived (*LEU2*-containing) plasmids were digested with *Bam*HI and *Hind*III, which theoretically generates the following fragments:

- empty G4AD: 5964 + 436 + 267 [bp]
- G4AD-Utp14: 5964 + 2410 + 981 [bp]

G4DBD derived (*URA3*-containing) plasmids were digested with *Bam*HI and *Sal*I, which theoretically generates the following fragments:

- empty G4DBD: 5985 + 12 [bp]
- G4DBD-Rlp24: 5985 + 606 [bp]

The agarose gel of this restriction analysis is shown in Figure 20.

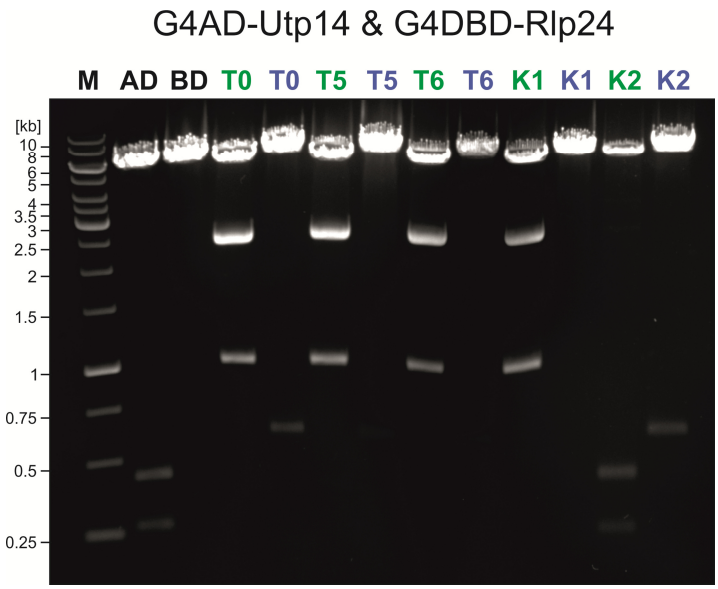

Figure 20: Restriction analysis of plasmids isolated from G4AD-Utp14 & G4DBD-Rlp24 transformants. 10 µl of each restriction assay was loaded on a 1% agarose gel. As a marker the Generuler 1kb DNA-ladder (Thermo Scientific) was used. AD and BD are purified G4AD and G4DBD plasmids without insert and were digested with *Bam*HI and *Hind*III (G4AD) or *Bam*HI and *Sal*I (G4DBD) and loaded as a control. G4AD (*LEU2* plasmids) and G4DBD (*URA3* palsmids) are labeled in green and blue, respectively. T0 (original from the transformant containing G4AD-Utp14 and G4DBD-Rlp24), K1 (original from the transformant G4AD-Utp14 and G4DBD), K2 (original from the transformant G4AD and G4DBD-Rlp24) are isolated from strains of the spotting assay in Figure 12. T5 and T6 of the transformant containing G4AD-Utp14 and G4DBD-Rlp24 are taken from the spotting assay in Figure 13.

The plasmid G4AD digested with *Bam*HI and *Hind*III generated a band of about 6 kbp, one band slightly below 0.5 kbp and a slight band at about 0.25 kbp. The G4DBD digested with *Bam*HI and *Sal*I generated a band at about 0.6 kbp. The 12 bp fragment was too small to be detected. The transformants T0, T5 and T6 of the G4AD-Utp14 + G4DBD-Rlp24 interaction study contain plasmids with the expected inserts. This can be argued by looking at the generated fragments which are of the right sizes: 5964 + 2410 + 981 [bp] for the G4AD plasmid containing Utp14 and 5985 + 606 [bp] fragments for the G4BDB plasmid containing Rlp24. However, the intensity of the 606 bp fragments of T5 and T6 were really weak. Only transformant T4 from the spotting assay Figure 13 was not able to lose either of the two plasmids. Therefore the plasmids could not be isolated and analysed.

Also the attempt to isolate plasmids of transformants of the interaction study between G4AD-Ecm16 and G4DBD-Tif6 which showed growth on histidine lacking media was not successful. The strains did not lose either one of the plasmids. The

only transformant that lost the plasmids was T3 from the dot spot in Figure 15. The restriction analysis showed that the strain was containing plasmids G4AD-Ecm16 and G4DBD-Tif6 (see Figure 21) although the strain was not able to grow on selective plates lacking histidine.

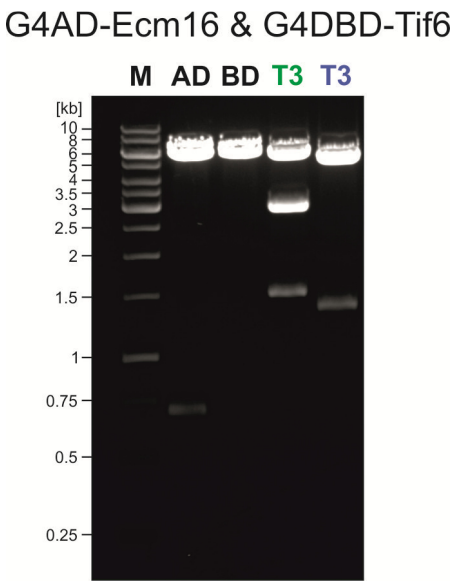

Figure 21: Restriction analysis of plasmids isolated from G4AD-Ecm16 & G4DBD-Tif6 transformant T3. 10 µl of each restriction assay was loaded on a 1% agarose gel. As a marker the Generuler 1kb DNA-ladder (Thermo Scientific) was used. AD and BD are purified G4AD and G4DBD plasmids without insert and were digested with *Hind*III (G4AD) or *Eco*RV (G4DBD) and loaded as a control. G4AD (*LEU2* plasmids) and G4DBD (*URA3* palsmids) are labeled in green and blue, respectively. T3 was isolated from the strain spotted in Figure 15.

For the restriction analysis of plasmids isolated from transformant T3 of the investigated interaction between Ecm16 and Tif6 (Figure 15) following restriction enzymes were chosen:

G4AD derived (*LEU2*-containing) plasmids were digested with *Hind*III, which theoretically generates the following fragments:

- empty G4AD: 5964 + 703 [bp]
- G4AD-Ecm16: 5964 + 2981 + 1514 [bp]

G4DBD derived (*URA3*-containing) plasmids were digested with *Eco*RV, which theoretically generates the following fragments:

- empty G4DBD: 5997 [bp]
- G4DBD-Tif6: 5355 + 1374 [bp]

As can be seen in Figure 21, the tested plasmids show the expected band sizes.

4. Discussion

4.1. Tandem affinity purification of the early Nop58 particle upon degradation of shuttling proteins

Before being able to purify and characterize Nop58 containing pre-ribosomal particles in strains depleted for selected shuttling proteins by the AID degradation system, the *NOP58* gene had to be tagged with the TAP tag. This was done by PCR amplification of the tag sequence with gene specific primers containing appropriate linker sequences and linear yeast transformation according to standard procedures [Longtine, et al., 1998]. The transformed strains already expressed shuttling protein AID fusions allowing their degradation in presence of auxin. These strains were kindly provided by Fasching, S. and are listed in Table 1. The tagging of Nop58 was then checked by colony PCR using appropriate primer pairs and by western blotting using a protein-A antibody (data not shown). In addition, Utp14 was provided with a HA tag using a similar strategy. This was necessary because no antibody against Utp14 is available and we didn't want to miss possible changes in appearance on the purified particle

The tagged strains were then tested for possible growth defects on YPD plates containing a concentration of 500 µM of the natural auxin IAA (indole-3-acetic acid). As can be seen in Figure 9 all tested strains except for the control lacking an AID tag as well as the strain expressing the Mrt4-AID fusion, showed a strong growth defect on auxin plates compared to YPD without auxin at 25°C as well as on 30°C. This indicates that the fusion proteins are efficiently degraded in the presence of auxin. *TIF6*, *NOG1* and *RLP24* are essential genes which explains the observed phenotypes. The strain expressing the Rlp24-AID fusion already showed a very strong growth defect on the plates without auxin. This indicates that a strong growth defect is caused by the C-terminal tagging of the protein.

In contrast, the strain with the Mrt4-AID fusion only showed a mild growth defect at 25°C in the presence of auxin. This indicated that the degradation of Mrt4 does not result in lethality but leads to a mild growth defect at lower temperatures. This

result is consistent with literature, showing that *MRT4* is a non-essential gene but its depletion causes a cold sensitive growth phenotype [Panse & Johnson, 2010].

We also studied the kinetics of degradation of the shuttling proteins in the presence of auxin. According to [Nishimura, et al., 2009] the degradation of AID-fusion proteins by the proteasome works better at lower temperatures which could also be observed in the dot spot in Figure 9. This is the reason why the incubation temperature for the following experiments was set to 25°C.

To investigate the time it takes for the AID fusion proteins to be degraded, cells were cultivated in a small volume and samples were taken after different treatment periods following the induction of the degradation process by auxin. Figure 10 shows the results of this experiment: the degradation of Tif6-AID and Mrt4-AID occurs within the first 15 minutes of treatment whereas the degradation of Nog1 and Rlp24 takes more time.

As already discussed, the AID tag was fused to the C-terminus of the proteins. C-terminal ends of Tif6 and Mrt4 are exposed on the surface of pre-60S particles [Wu, et al., 2016] making the AID tag accessible for the proteasome which would explain the rapid onset of the effect. Despite the fast onset of tagged proteins the strains expressing the Mrt4-AID and Tif6-AID fusions showed growth rates comparable to the control strain lacking the AID tag.

The complete degradation of Nog1-AID and Rlp24-AID took more time, up to 90 minutes. For Nog1, this slower degradation could be explained by the topology of the protein on the pre-60S particle, which exposes its C-terminal helix into the polypeptide exit channel. Therefore, the AID tag might be less accessible, explaining the slower kinetics of degradation. In addition, tagging of this part of the protein could interfere with the function of the protein leading to slower growth rates. Indeed, the Nog1-AID strain exhibits slower growth rates as compared to Mrt4 and Tif6. In the Rlp24-AID strain the tagging at the C-terminal end showed the most severe growth defect, leading to cell division times of about 7 to 8 hours (data not shown). These defects indicate that the C-terminal end of Rlp24 plays a

crucial role for the function of the protein. Since this part of Rlp24 is recognized by Drg1, it would be interesting to test, whether the slow growth phenotype of the Rlp24-AID strain is related with the activity of the AAA-ATPase.

For the following tandem affinity purification an incubation time of 30 minutes was chosen for the auxin treatment to not raise unspecific effects due to prolonged inhibition of the pathway.

In Figure 11 the results of the depletion of shuttling proteins on the composition of Nop58-TAP containing pre-ribosomal particles is shown. The SDS-PAGE showed that the purification worked well for most of the samples. In all lanes the same amount of protein was applied according to the cbp signal in a preliminary western blot (data not shown). However, the Rlp24-AID fusion only showed weak bands for co-purifying proteins. This finding suggests that the tag on Rlp24 has a pronounced effect on Nop58-TAP loading on the pre-ribosomal particle. Although several protein bands (for example those marked with a star in Figure 11A) differed between the individual strains and/or between auxin treated and untreated strains, a two-step purification followed by mass spectrometry identification of proteins differing in the samples would lead to a clearer picture.

Western blot analysis of the tandem affinity purification showed that the level of the bait protein Nop58 was almost the same in all lanes which means that the protein amounts were well adjusted. The western blot with the anti-Flag antibody detecting the AID fusion proteins showed that Tif6-AID and Mrt4-AID were completely degraded after 30 minutes. In contrast, only about half of Nog1-AID was degraded during the same treatment period. Interestingly, the amount of Rlp24-AID was only slightly reduced after 30 minutes of treatment, again suggesting that the tag interferes with degradation of the protein.
The membrane was also probed with an anti-HA antibody to detect Utp14. This protein was shown to recruit and activate the RNA helicase Ecm16 which unwinds the U3 snoRNA from the 90S ribosome [Zhu, et al., 2016]. In the samples of Rlp24-AID hardly any Utp14 could be detected which indicates that Nop58 and therefore U3 snoRNP cannot be properly loaded onto pre-ribosomal particles.

The decreasing amounts of Utp14, Noc1, Noc2 and Rrp12 in the untreated samples of Tif6-AID and Nog1-AID suggest that the AID tag is interfering with the loading of these proteins onto Nop58 containing early pre-ribosomes. Previous studies have shown that depletion of Nog1 leads to defects in 60S subunit biogenesis [Saveanu, et al., 2003; Jensen, et al., 2003]. In this work a disruption of early binding proteins was observed by introduction of a tag on the C-terminal end of the protein. Also the tag on Tif6 seems to disturb the processing and maturation of pre-ribosomal particles.

However, small differences of band intensities need to be interpreted very carefully because the protein amount is not adjusted to 100% which could lead to misinterpretation. What can be said with certainty is that the purification of the Nop58 particle in the strain expressing the Rlp24-AID contained much less co-purifying pre-ribosome maturation factors.

For Rlp24-AID 30 minutes of auxin treatment was not enough to be degraded, as seen in Figure 6B, although the C-terminus of Rlp24 is exposed on the surface of the particles [Wu, et al., 2016]. Nevertheless, the strain exhibited a really slow proliferation, needing nearly 8 hours for its cells to duplicate. An explanation of the strong growth inhibition induced by the AID tagging of Rlp24 might be that the C-terminal tag gets masked and is not that accessible for the AAA-ATPase Drg1 to promote the maturation of pre-60S particles. This might lead to a disruption of ribosome assembly leading to a deceleration of growth and cell division. Since Rlp24 is a shuttling protein and is released by Drg1 in the cytoplasm, it would be interesting to determine the localization of the AID tagged Rlp24. If the tag interferes with the release reaction catalysed by Drg1, it might preferentially accumulate in the cytoplasm, causing depletion of the protein in the nucleus. Nevertheless, the strong decrease of all proteins in the Nop58-TAP purifications from the Rlp24-AID strain indicates an important role of Rlp24 in the loading of U3 snoRNP onto the pre-ribosomal particle or assembly of the U3 snoRNP.

To get an inside into the effect of Rlp24 on U3 snoRNP function, rRNA isolation and investigation of the RNA species by northern blotting will be the next step in

this project to monitor the effects on rRNA processing. Also the whole purification should be carried out as a two-step purification combined with mass spectrometry to confirm the results.

Taken together, these results enforce the assumption of shuttling proteins being involved in early ribosome maturation events.

4.2. Y2H interaction network between 90S and 60S pre-ribosomal factors

The first step of creating an interaction network between Utp14 and shuttling proteins as well as Ecm16 and shuttling proteins was to clone the genes encoding for these proteins into Y2H vectors. These vectors contain either the Gal4 activation (pGAD-C1) or the Gal4 DNA binding domain (pGBDU-C1) followed by multiple cloning sites (MCS) and a transcription terminator sequence. The correct insertion of genes into the plasmids was verified by restriction analysis and sequence analysis. Strains expressing AD-Utp14 fusion and different shuttling proteins fused with the DNA-binding domain in the Y2H reporter strain PJ69-4A were tested for activation of the *HIS3* reporter gene in the presence or absence of 3-amino-1,2,4-triazole. 3-AT is a competitive inhibitor to the *HIS3* gene product imidazoleglycerol-phosphate dehydratase which raises the minimum amount of *HIS3* expression needed for the cells to survive and thus reduces unspecific interaction [Caufield, et al., 2012].

Looking at the spotting assays in Figure 12 & Figure 13 of the investigated interaction between Utp14 and Rlp24 no conclusive answer whether there is an interaction or not can be provided because not all transformants show the same phenotype. In sum, only two out of 7 spotted transformants were able to grow. Unfortunately thorough attempts to find the reason for this heterogenity were not successful. The sequences of the constructed plasmids were correct (chapter 3.3.1) and the restriction analysis of isolated plasmids showed that growing as well as non-growing transformants contained both plasmids expressing the required fusion proteins (chapter 3.3.2). What could still be done to explain why the

transformants showed a different phenotype is to sequence the isolated plasmids which were used for restriction analysis. This might reveal mutations in the coding sequence leading to the expression of a different fusion protein.

The investigated interaction between G4AD-Ecm16 and G4DBD-Tif6 was inconclusive. The slight growth of 3 out of 7 tested transformants on SD-Leu-Ura-His plates suggests an interaction (see Figure 14 & Figure 15) but raises the question why not all of them were able to grow. Checking the sequence of the constructed plasmids showed that the cloning was successful (Figure 18 & Figure 19). The genes were ligated into the plasmids correctly without any differences to the sequences which were predicted by the Serial Cloner program. The genes were inserted in frame to the prior activation and binding domain sequences. Isolation and restriction analysis of the G4AD-Ecm16 and G4DBD-Tif6 plasmids could not be executed due to the inability of most strains to lose the plasmids. From one transformant which was not able to grow on selective plates lacking histidine the *LEU2* as well as the *URA3* plasmid could be isolated and restriction analysis showed the G4AD-Ecm16 and the G4DBD-Tif6 plasmid both were present in the strain.

The finding that no plasmids could be isolated from growing strains raises the possibility that the strains do in fact not contain the plasmids. An explanation for the growth might be a genomic mutation allowing it to grow on selective plates without carrying the plasmids. This could be verified by sequencing the whole genome of the strains. But first the experiment should be repeated.

Although the Y2H analysis was inconclusive the *in vitro* interaction between Utp14 and Rlp24 (Fasching, S. unpublished results) supports the hypothesis that they interact *in vivo*. This would be the first discovery of a 60S shuttling factor involved in 90S pre-ribosome formation and assembly.

5. References

Beltrame, M., Henry, Y., & Tollervey, D. (1994). Mutational analysis of an essential binding site for the U3 snoRNA in the 5' external transcribed spacer of yeast pre-rRNA. *Nucleic Acids Res*, Nov;25(22823):5139-47.

Caufield, J. H., Sakhawalkar, N., & Uetz, P. (2012). A comparison and optimization of yeast two-hybrid systems. *Methods*, Dec;58(4):317-24.

Chaker-Margot, M., Barandun, J., Hunziker, M., & Klinge, S. (2016). Architecture of the yeast small subunit processome. *Science*, Dec15,pii:aal1880.

Chaker-Margot, M., Hunziker, M., Barandun, J., Dill, B. D., & Klinge, S. (2015). Stage-specific assembly events of the 6-MDa small-subunit processome initiate eukaryotic ribosome biogenesis. *Nat Struct Mol Biol*, Nov;22(11):920-3.

Dragon, F., Gallagher, J. E., Compagnone-Post, P. A., Mitchell, B. M., Porwancher, K. A., Wehner, K. A., et al. (2002). A large nucleolar U3 ribonucleoprotein required for 18S ribosomal RNA biogenesis. *Nature*, Jun27;417(6892):967-70.

Dutca, L. M., Gallagher, J. E., & Baserga, S. J. (2011). The initial U3 snoRNA:pre-rRNA base pairing interaction required for pre-18S rRNA folding revealed by in vivo chemical probing. *Nucleic Acids Res*, Jul;39(12):5164-80.

Fatica, A., Oeffinger, M., Dlakic, M., & Tollervey, D. (2003). Nob1p is required for cleavage of the 3' end of 18S rRNA. *Mol Cell Biol*, Mar;23(5):1798-807.

French, S. L., Osheim, Y. N., Cioci, F., Nomura, M., & Beyer, A. L. (2003). In exponentially growing *Saccharomyces cerevisiae* cells, rRNA synthesis is determined by the summed RNA polymerase I loading rate rather than by the number of active genes. *Mol Cell Biol*, Mar;23(5):1558-68.

Gasse, L., Flemming, D., & Hurt, E. (2015). Coordinated Ribosomal ITS2 RNA Processing by the Las1 Complex Integrating Endonuclease, Polynucleotide Kinase, and Exonuclease Activities. *Mol Cell*, Dec3;60(5)808-15.

Geerlings, T. H., Vos, J. C., & Raué, H. A. (2000). The final step in the formation of 25S rRNA in *Saccharomyces cerevisiae* is performed by 5'->3' exonucleases. *RNA*, Dec;6(12)1698-703.

Gietz, R. D. (2014). Yeast transformation by the LiAc/SS carrier DNA/PEG method. *Methods Mol Biol*, 1205:1-12.

Henry, Y., Wood, H., Morrissey, J. P., Petfalski, E., Kearsey, S., & Tollervey, D. (1994). The 5' end of yeast 5.8S rRNA is generated by exonucleases from an upstream cleavage site. *EMBO J*, May:15;13(10):2452-63.

Horn, D. M., Mason, S. L., & Karbstein, K. (2011). Rc1 Protein, a Novel Nuclease for 18S Ribosomal RNA Production. *J Biol Chem*, DOI 10.1074/jbc.M111.268649.

James, P., Halladay, J., & Craig, E. A. (1996). Genomic Libraries and a Host Strain Designed for Highly Efficient Two-Hybrid Selection in Yeast. *Genetics*, 144:1425-1436.

Jensen, B. C., Wang, Q., Kifer, C. T., & Parsons, M. (2003). The NOG1 GTP-binding protein is required for biogenesis of the 60S ribosomal subunit. *J Biol Chem*, Aug22;278(34):32204-11.

Kappel, L., Loibl, M., Zisser, G., Klein, I., Fruhmann, G., Gruber, C., …, Bergler, H. (2012). Rlp24 activates the AAA-ATPase Drg1 to initiate cytoplasmatic pre-60S maturation. *J Cell Biol*, Nov26;199(5):771-82.

Kemmler, S., Occhipinti, L., Veisu, M., & Panse, V. G. (2009). Yvh1 is required for a late maturation step in the 60S biogenesis pathway. *J Cell Biol,* Sep21;186(6):863-80

Kornprobst, M., Turk, M., Kellner, N., Cheng, J., Flemming, D., Koš-Braun, I., …, Hurt, E. (2016). Architecture of the 90S Pre-ribosome: A Structural View on the Birth of the Eukaryotic Ribosome. *Cell*, Jul14;166(2):380-93.

Kos, M., & Tollervey, D. (2010). Yeast pre-rRNA processing and modification occur cotranscriptionally. *Mol Cell*, Mar26;37(6):809-20.

Lo, K. Y., Li, Z., Bussiere, C., Bresson, S., Marcotte, E. M., & Johnson, A. W. (2010). Defining the pathway of cytoplasmatic maturation of the 60S ribosomal subunit. *Mol Cell*, Jul30;39(2):196-208.

Lo, K. Y., Li, Z., Wang, F., Marcotte, E. M., & Johnson, A. W. (2009). Ribosome stalk assembly requires the dual-specificity phosphatase Yvh1 for the exchange of Mrt4 with P0. *J Cell Biol*, Sep21;186(6):849-62.

Loibl, M., Klein, I., Prattes, M., Schmidt, C., Kappel, L., Zisser, G., …, Bergler, H. (2014). The drug diazaborine blocks ribosome biogenesis by inhibiting tha AAA-ATPase Drg1. *J Biol Chem*, Feb14;289(7):3913-22.

Longtine, M. S., McKenzie, A. 3., Demarini, D. J., Shah, N. G., Wach, A., …, Pringle J. R. (1998). Additional modules for versatile and economical PCR-based gene deletion and modification in *Saccharomyces cerevisiae*. *Yeast*, Jul;14(10):953-61.

Lygerou, Z., Allmang, C., Tollervey, D., & Séraphin, B. (1996). Accurate processing of a eukaryotic precursor ribosomal RNA by ribonuclease MRP in vitro. *Science*, Apr12;272(5259):268-70.

Mitchell, P., Petfalski, E., & Tollervey, D. (1996). The 3' end of yeast 5.8S rRNA is generated by an exonuclease processing mechanism. *Genes Dec*, Feb:15;10(4):502-13.

Nishimura, K., Fukagawa, T., Takisawa, H., Kakimoto, T., & Kanemaki, M. T. (2009). An auxin-based degron system for the rapid depletion of proteins in nonplant cells. *Nat Methods*, Dec;6(12)917-22.

Oeffinger, M., Zenklusen, D., Ferguson, A., Wei, K. E., El Hage, A., Tollervey, D., …, Rout, M. P. (2009). Rrp17p is a eukaryotic exonuclease required for 5' end processing of Pre-60S ribosomal RNA. *Mol Cell*, Dec11;36(5):768-81.

Osheim, Y. N., French, S. L., Keck, K. M., Champion, E. A., Spasov, K., ..., Beyer, A. L. (2004). Pre-18S ribosomal RNA is structurally compacted into the SSU processome prior to being cleaved from nascent transcripts in *Saccharomyces cerevisiae*. *Mol Cell*, Dec22;16(6):943-54.

Panse, V. G., & Johnson, A. W. (2010). Maturation of eukaryotic ribosomes: acquisition of functionality. *Trends Biochem Sci*, May;35(5):260-6.

Pertschy, B., Saveanu, C., Zisser, G., Lebreton, A., Tengg, M., Jacquier, A., …, Bergler, H. (2007). Cytoplasmatic recycling of 60S preribosomal factors depends on the AAA protein Drg1. *Mol Cell Biol*, Oct;27(19):6581-92.

Pertschy, B., Schneider, C., Gnädig, M., Schäfer, T., Tollervey, D., & Hurt, E. (2009). RNA helicase Prp43 and its co-factor Pfa1 promote 20 to 18 S rRNA processing catalyzed by the endonuclease Nob1. *J Biol Chem*, Dec11;284(50):35079-91.

Pertschy, B., Zisser, G., Schein, H., Köffel, R., Rauch, G., Grillitsch, K., …, Bergler, H. (2004). Diazaborine treatment of yeast cells inhibits maturation of the 60S ribosomal subunit. *Mol Cell Biol*, Jul;24(14):6476-87.

Puig, O., Caspary, F., Rigaut, G., Rutz, B., Bouveret, E., Bragado-Nilsson, E., …, Séraphin, B. (2001). The tandem affinity purification (TAP) method: a general procedure of protein complex purification. *Methods*, Jul;24(3):218-29.

Rigaut, G., Shevchenko, A., Rutz, B., Wilm, M., Mann, M., & Séraphin, B. (1999). A generic protein purification method for protein complex characterization and proteome exploration. *Nat Biotechnol*, Oct;17(10):1030-2.

Sardana, R., Liu, X., Granneman, S., Zhu, J., Gill, M., Papoulas, O., …, Johnson, A. W. (2015). The DEAH-box helicase Dhr1 dissociates U3 from the pre-rRNA to promote formation of the central pseudoknot. *PLoS Biol*, Feb24;13(2):e1002083.

Sarkar, A., Pech, M., Thoms, M., Beckmann, R., & Hurt, E. (2016). Ribosome-stalk biogenesis is coupled with recruitment of nuclear-export factor to the nascent 60S subunit. *Nat Struct Mol Biol*, Dec;23(12):1074-1082.

Saveanu, C., Namane, A., Gleizes, P. E., Lebreton, A., Rousselle, J. C., …, Fromont-Racine, M. (2003). Sequential protein association with nascent 60S ribosomal particles. *Mol Cell Biol*, Jul;23(13):4449-60.

Senger, B., Lafontaine, D. L., Graindorge, J. S., Gadal, O., Camasses, A., …, Fasiolo, F. (2001). The nucle(ol)ar Tif6p and Efl1p are required for a late cytoplasmatic step of ribosome synthesis. *Mol Cell*, Dec;8(6):1363-73.

Sun, Q., Zhu, X., Qi, J., An, W., Lan, P., Tan, D., ..., Ye, K. (2017). Molecular architecture of the 90S small subunit pre-ribosome. *Elife*, Feb28;6. pii: e22086. doi: 10.7554/eLife.22086.

Talkish, J., Biedka, S., Jakovljevic, J., Zhang, J., Tang, L., Strahler, J. R., ..., Woolford, J. L. Jr. (2016). Disruption of ribosome assembly in yeast block cotranscriptional pre-rRNA processing and affects the global hierarchy of ribosome biogenesis. *RNA*, Jun;22(6):852-66.

Thoms, M., Thomson, E., Baßler, J., Gnädig, M., Griesel, S., & Hurt, E. (2015). The Exosome Is Recruited to RNA Substrates through Specific Adaptor Proteins. *Cell*, Aug27;162(5):1029-38.

Turowski, T. W., & Tollervey, D. (2015). Cotranscriptional events in eukaryotic ribosome synthesis. *Wiley Interdiscip Rev RNA*, Jan-Feb;6(1):129-39.

Udem, S. A., & Warner, J. R. (1972). Ribosomal RNA synthesis in *Saccharomyces cerevisiae*. *J Mol Biol*, Mar28;65(2):227-42.

Venema, J., & Tollervey, D. (1995). Processing of pre-ribosomal RNA in *Saccharomyces cerevisiae*. *Yeast*, Dec;11(16):1629-50.

Warner, J. R. (1999). The economics of ribosome biosynthesis in yeast. *Trends Biochem. Sci*, 24:437-440.

Woolford, J. L. Jr., & Baserga, S. J. (2013). Ribosome biogenesis in the yeast *Saccharomyces cerevisiae*. *Genetics*, Nov;195(3):643-81.

Wu, S., Tutuncuoglu, B., Yan, K., Brown, H., Zhang, Y., Tan, D., ..., Gao, N. (2016). Diverse roles of assembly factors revealed by structures of late nuclear pre-60S ribosomes. *Nature*, Jun2;534(7605):133-7.

Zhang, L., Lin, J., & Ye, K. (2013). Structural and functional analysis of the U3 snoRNA binding protein Rrp9. *RNA*, May;19(5):701-11.

Zhu, J., Liu, X., Anjos, M., Correll, C. C., & Johnson, A. W. (2016). Utp14 recruits and activates the RNA helicase Dhr1 to undock U3 snoRNA from the pre-ribosome. *Mol Cell Biol*, Jan4. pii: MCB.00773-15.